university of groningen

faculty of mathematics and natural sciences

Understanding the dynamics of wind-driven ocean circulation

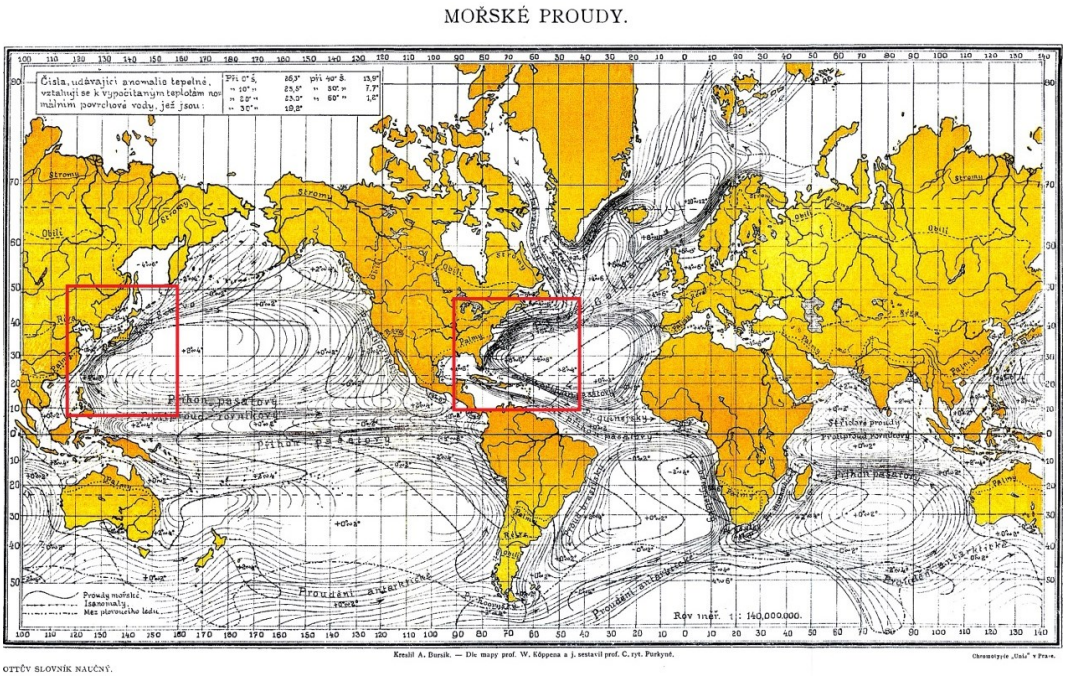

Bachelor Project Mathematics and Physics

July 2015

Student: R.M. Ledoux

First supervisor: Dr. B. Carpentieri

Second supervisor: Dr. T.L.C. Jansen

Cover picture by Cyrill Purkyně and A. Bursík, taken from [7], showing westward intensification of streamlines inside the red boxes (drawn by the author).

ABSTRACT

This thesis describes several simple models of ocean flows, such as the Stommel model and the Munk model. Some physical and mathematical background is given on the concepts and equations of fluid dynamics, of which the Navier-Stokes equations are of biggest importance. These equations will be adapted to describe flows in a rotating spherical coordinate system that is applicable to large-scale flows on planet Earth and other planets.

In order to make the models of interest analytically solvable, some simplifications are introduced. The curved planet's surface is, for instance, approximated by a tangent plane. The equations of Henry Stommel's Gulf Stream model are introduced and solved analytically. A more general approach to model ocean streams derived by Joseph Pedlosky is also introduced, from which both the Stommel model and the Munk model, another important model by Walter Munk, can be obtained. Finally, Pedlosky's method is used to introduce time-dependent tidal forces into the time-independent Stommel model. Several graphs and MATLAB scripts are included to visualize the models.

CONTENTS

1

INTRODUCTION

In the field of *Fluid Dynamics*, models of any kind of fluid flow are studied and developed. It thus has physical applications, but also has very mathematical aspects: some simple models can be solved analytically by applying, for instance, Fourier methods and separation of variables to solve differential equations, whereas other models only allow for numerical solutions, by their complexity.

The goal of this thesis is to study the effect of Coriolis force on particle motion in a fluid flow, that comes into play when large-scale flows in a rotating system are considered, such as the Gulf Stream.

In Chapter 2 the relevant *physical quantities* of Fluid Dynamics are introduced and shortly explained. Several models for describing a flow will be introduced in Chapter 3 and it will be shown that they are equivalent. The *Navier-Stokes equations*, a system of differential equations describing the dynamics of fluid flows, will be derived and useful concepts such as the *substantial derivative* and *stream functions* are introduced.

In Chapter 4, a coordinate transformation will be applied to the Navier-Stokes equations to find their counterparts in a rotating spherical coordinate system. Due to this transformation, some extra terms appear in the equations, that represent a pseudo force called the *Coriolis effect*, which is experienced due to the rotation. The use of this rotating system is necessary for large-scale systems on Earth. When working with a spherical coordinate system, one has to cope with many nonlinearities and curved surfaces that are relatively complicated to calculate with. Therefore, it is sometimes easier to approximate areas of the planet surface by a tangent plane, a method called the β*-plane approximation*, which is presented in the last section of this chapter.

In the next chapter, Chapter 5, some approximations are given to describe fluid flows in shallow water, which give rise to the *shallow water equations*.

In Chapter 6, some first simple flow models are studied.

The model of Henry Stommel was derived to explain the *cumulation of streamlines* that appears along the western boundary of large-scale ocean flows such as the Gulf Stream. Stommel's model, that is presented in Chapter 7, describes a simplified linear model of a flow in a rectangular basin, but definitely shows this cumulation.

Chapter 8 states the ocean model of Walter Munk, that is in many respects very similar to the Stommel model, and gives a more *general method of derivation* introduced by Joseph Pedlosky,

that uses a series expansion and can also be used to find and solve more accurate higher order models.

The general model of Pedlosky is used in the last chapter, Chapter 9, to extend the (time-independent) Stommel model to a time-dependent model that deals with the tidal force exerted by a satellite such as the moon.

In the Appendices, several MATLAB scripts are included that reproduce graphs and simulations presented in this work.

2

CONCEPTS OF FLUID DYNAMICS

The goal of this thesis is to describe some effect in a physical system: the impact of Coriolis force on the behaviour of fluid motion. Any physical system is described by its physical quantities. This chapter is dedicated to defining the physical quantities of our system, the main four of which are pressure, density, temperature and flow velocity. Since these will be common terms to most physicists, they will only be discussed shortly.

Besides these quantities, some other basal concepts will be introduced in the following sections. The notions being introduced and discussed in this chapter are mainly taken from [2, ch. 1], which could be read by anyone seeking for more background information.

2.1 PHYSICAL QUANTITIES

2.1.1 *Pressure*

The physical quantity *pressure* represents the amount of normal force per unit area on some surface. This surface can either be a *real surface* (the surface of an object), or some (artificial) *free surface*, defined somewhere in space. Pressure (denoted p) can be defined mathematically at any point of a surface as

$$p := \frac{dF}{dA}, \tag{2.1}$$

where dA denotes a local infinitesimal element of the surface and dF is the normal force acting on the surface element dA. Since force equals the time derivative of momentum, pressure can physically be seen as the change of momentum per cross-sectional area per unit time. In SI units, this scalar quantity is expressed in newtons per square meter (Nm^{-2}) or pascals (Pa).

2.1.2 *Density*

In physics, density is a quantity that describes the amount of mass per unit volume. We can define this quantity locally by giving this mass-volume ratio in an infinitesimal volume element. The density, indicated by ρ, of any substance in three dimensional space can thus be defined at any fixed point as

$$\rho := \frac{dm}{dV}, \tag{2.2}$$

where dm is the (infinitesimal) amount of mass contained in the infinitesimal volume dV. Density is also a scalar quantity, expressed in kilograms per qubic meter (kgm^{-3}).

2.1.3 *Temperature*

The random motion of molecules strongly correlates with their temperature. At high temperatures, the velocity of random motion is much higher than at lower temperatures. Temperature T, a scalar quantity expressed in Kelvins (K), is calculated from the (local) mean kinetic energy E_k and the Boltzmann constant k, by

$$E_k = \frac{3}{2}kT, \tag{2.3}$$

an equation known from thermodynamics. In more sophisticated models, temperature differences between regions in the flow may play an important role. However, the models presented later on in this work in general ignore any temperature dependency.

2.1.4 *Flow velocity*

The last fundamental quantity we will introduce is the *flow velocity*. The flow velocity physically represents the velocity of a small volume in the flow and is defined mathematically as the average velocity of particles in an infinitesimal fluid element of a flowing liquid or gas at any fixed point in space. Whereas pressure, density and temperature are all scalar quantities, since any velocity can have both magnitude and direction, the flow velocity is a vector and it is denoted[1] as $\boldsymbol{V}$.

In a steady flow, the particle orbits are continuous and velocities do not depend on time explicitly.

2.2 FORCES AND TORQUES

In computational fluid dynamics, forces acting on a body are divided into two distinct groups: forces that act from a distance, such as gravitational and electrical forces, and forces that act directly on the surface of an object, for instance the force due to pressure. Without saying anything specific about their origin, we can group these first forces, which are called *body forces*, into a single quantity $\boldsymbol{f}$, which is the amount of body force per unit mass. We will come back to the body force later on.

Forces acting on the surface of the body are called *surface forces*. We can distinguish between *pressure distribution*, which is related to normal forces, and *shear stress distribution*, related to forces tangential to the body surface. The shear stress τ has the same dimensions as

1 Throughout this thesis, scalar quantities are printed in normal weight, whereas vector quantities are printed in **boldface**. Sets are also labelled in normal weight.

pressure p. Pressure p and stress τ give rise to a force due to surface forces R and a torque M on the body.

2.3 APPROXIMATIONS/TYPES OF FLOWS

In order to make flow models more easy to solve, it may be helpful to assert certain approximations. Unless stated otherwise, the following approximations are assumed in all models that will be discussed.

Continuity Although any real flow actually consists of a finite number of separate particles, in general fluids are so dense and the length scales of the models are so large that the fluid can be considered to be a *continuum*.

Inviscidity *Viscosity* is a physical quantity that represents the shear stress between particles in a fluid. When the Reynolds number is high, as it is for ocean-like streams[2], the fluid can accurately be modelled as an inviscid flow, such that shear stress between fluid particles can be ignored.

Incompressibility When a liquid is *incompressible*, its Mach number is low[3] ($M \ll 1$) and the density is constant throughout the fluid (it is homogeneous). Though in reality different layers of the ocean will have different densities, models become much more simple when this property is ignored. The low Mach number implies a *subsonic flow* which has smooth streamlines and disturbances that are felt throughout the entire flow field, in contrast to supersonic flow.

In reality, there exist no flows that are fully continuous, inviscid or incompressible, but the ocean flows under discussion approximate these properties closely. Models can be created and exist that do not assume these properties, but in general they require a much more advanced set of equipment to be solved. Imagine for instance modelling a fluid by considering all individual fluid particles separately, instead of viewing the fluid as a continuum. For small samples of a low-density gas it would be doable, but the number of particles in 1 ml water is already of the order of 10^{22}, too much probably even for the best computers.

The quantities introduced in this chapter, the most important of which are *pressure* p, *flow density* ρ and *flow velocity* $\boldsymbol{V}$, and the approximations of *continuity*, *inviscidity* and *incompressibility* will be used in the next chapter in the derivation of the equations of fluid dynamics.

2 The Reynolds number is defined as the ratio of *inertial* or *external forces* to *viscous forces* and is proportional to the dimensions of the stream, which are of course large in the oceans.

3 The Mach number is defined as the ratio of the flow speed to the speed of sound in the medium.

3

EQUATIONS OF FLUID DYNAMICS

In this chapter, first you will read about several ways a fluid can be modelled, and then the fundamental equations of fluid dynamics are introduced and discussed. These equations are based on the physical principles of mass conservation, energy conservation and Newton's second law.

The introduction of models, concepts and equations in this chapter mainly follows the line of Anderson in [1], and for a more firm explanation and full derivations of the concepts and formulas the reader is referred to this book.

3.1 MODELS

In fluid dynamics there exist four commonly used ways to model a continuum fluid. This section shortly describes all those four models.

3.1.1 *Fixed finite control volume* (FFCV)

The first model to describe a continuum flow, is a method that uses a *finite control volume fixed in space* and studies the fluid moving through it. The finite control volume is in this case a fixed volume $\mathscr{V}$ in space, and its surface S is called the *control surface*.

The physical principles of fluid dynamics are applied to the part of the fluid inside the volume and the flow through the boundary of the volume, to find the equations that describe the dynamics of the fluid. From now on, we will refer to this model as FFCV.

3.1.2 *Moving finite control volume* (MFCV)

The second model uses, as the above one, a finite control volume $\mathscr{V}$. However, this time the volume is not fixed in space, but it shape and position evolve in such a way that the particles inside the volume remain the same particles as time elapses. The *control surface* S is again the surface of the control volume and the equations of fluid dynamics are again found by applying the appropriate physical principles. This model will be referred to as MFCV.

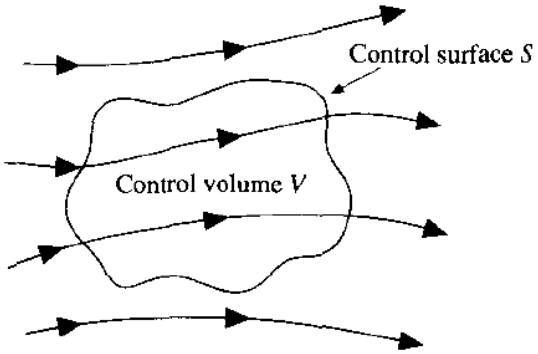

(a) *The fixed finite control volume.*

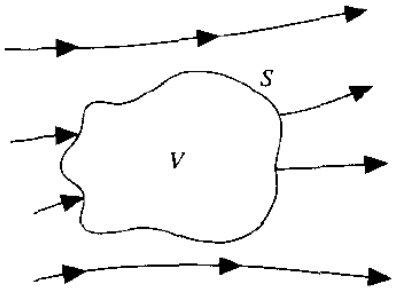

(b) *The moving finite control volume.*

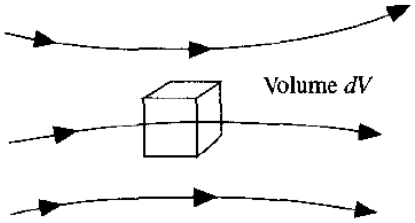

(c) *The fixed infinitesimal fluid element.*

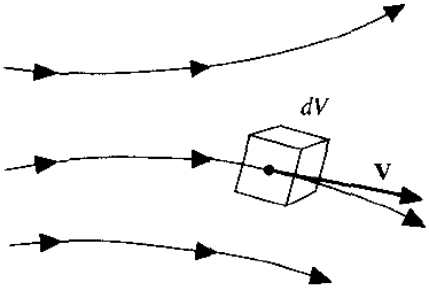

(d) *The moving infinitesimal fluid element.*

Figure 1.: *The four fluid models. Pictures taken from [1]*

3.1.3 *Fixed infinitesimal fluid element* (FIFE)

The third model we describe is very similar to the first one. The main difference is that instead of a finite control volume, an *infinitesimal fluid element* $d\mathcal{V}$ is used. Physically, this does only make sense if the fluid is considered to be a continuum. This fluid element is fixed in space and physical principles are applied to it to find the dynamics of the flow. We denote this model as FIFE.

3.1.4 *Moving infinitesimal fluid element* (MIFE)

The last model that is of importance regards a infinitesimal element $d\mathcal{V}$ that is moving with the flow velocity along a *streamline*. Again the dynamics of the flow can be found by application of the physical principles to this element. The name of this model is abbreviated to MIFE.

3.2 THE SUBSTANTIAL DERIVATIVE

When we consider a moving infinitesimal fluid element as in the MIFE model, and denote the velocity vector of this element by $\boldsymbol{V}$, we can define the *substantial derivative*, labelled $\frac{D}{Dt}$, as

$$\frac{D}{Dt} := \underbrace{\frac{\partial}{\partial t}}_{\text{local derivative}} + \underbrace{(\boldsymbol{V}\cdot\nabla)}_{\text{convective derivative}} . \tag{3.1}$$

Physically, the substantial derivative of a quantity can be seen as the time rate of change of that quantity following the moving element (see [1, pp. 47-49] for a derivation). The first term ($\frac{\partial}{\partial t}$) denotes the *local derivative*, because of local fluctuations with respect to time. The second term ($\boldsymbol{V}\cdot\nabla$), is called the *convective derivative* and denotes the rate of change due to the movement of the fluid element.

Mathematically, we can write for any scalar function F:

$$\begin{aligned}\frac{DF}{Dt} &= \frac{\partial F}{\partial t} + \boldsymbol{V}\cdot\nabla F \\ &= \frac{\partial F}{\partial t} + \frac{dx}{dt}\frac{\partial F}{\partial x} + \frac{dy}{dt}\frac{\partial F}{\partial y} + \frac{dz}{dt}\frac{\partial F}{\partial z} \\ &= \frac{dF}{dt}.\end{aligned}$$

Thus, mathematically speaking, the substantial derivative is just the *total derivative* with respect to time. It is of importance since it appears frequently in equations we will introduce or derive.

The substantial derivative can be applied to *vector functions* by applying it to all vector elements, giving the time derivative of the vector.

3.3 DIVERGENCE OF THE VELOCITY

Another term that appears frequently throughout in computational fluid dynamics, and also in the rest of this thesis, is the *divergence of the velocity*, $\nabla\cdot\boldsymbol{V}$. This divergence can mathematically be written on using an infinitesimally small fluid element $\delta\mathscr{V}$ as

$$\nabla\cdot\boldsymbol{V} = \frac{1}{\delta\mathscr{V}}\frac{D(\delta\mathscr{V})}{Dt}. \tag{3.2}$$

Physically, this divergence represents the time rate of change of the volume of a moving fluid element per unit volume.

3.4 THE NAVIER-STOKES EQUATIONS

As mentioned earlier, the equations that describe the dynamics of a fluid are based on three key physical principles: mass conservation, energy conservation and Newton's second law.

These three principles lead to a system of equations which are together called the *Navier-Stokes equations*[1].

In principle, any of the four models described above could be used to derive the Navier-Stokes equations. They give rise to different forms of the same equations. We state the equations here accompanied by some small derivations and refer to [1] for a full derivation.

3.4.1 *The continuity equation*

The principle of mass conservation is applied to any of the fluid models in Section 3.1 to find different forms of the *continuity equation*. We will briefly discuss and state the versions that follow from the various models and sketch how they are related.

3.4.1.1 *In the* FFCV *model*

Mass conservation implies that mass does not simply disappear. Thus when the amount of mass inside a fixed control volume $\mathcal{V}$ increases, it physically means there must occur a mass flow equal through the surface S of the control volume $\mathcal{V}$. The mass flow through any fixed surface is equal to the product of the density times the component of velocity perpendicular to the surface times the area of the surface. Over an infinitesimal surface element $d\boldsymbol{S}$ (pointing in direction outward of the control volume), this can be written as $\rho \boldsymbol{V} \cdot d\boldsymbol{S}$. Integration over the whole surface gives the total mass flow through S. In this orientation (with $d\boldsymbol{S}$ pointing outward), this must equal the decrease of mass inside $\mathcal{V}$, in integral form (*the continuity equation*):

$$\underbrace{\frac{\partial}{\partial t}\left[\iiint_{\mathcal{V}} \rho \, d\mathcal{V}\right]}_{\text{mass increase inside volume}} + \underbrace{\oiint_{S} \rho \boldsymbol{V} \cdot d\boldsymbol{S}}_{\text{net mass flow out of control volume}} = 0. \tag{3.3}$$

3.4.1.2 *In the* MFCV *model*

Due to mass conservation, in the MFCV model, the mass in the control volume is constant, since it is defined as the volume containing a certain set of particles. The mass inside the control volume $\mathcal{V}$ equals $\iiint_{\mathcal{V}} \rho \, d\mathcal{V}$, and so its substantial derivative is zero, which gives the continuity equation:

$$\frac{D}{Dt} \iiint_{\mathcal{V}} \rho \, d\mathcal{V} = 0. \tag{3.4}$$

There is no mass flow through the control surface S.

3.4.1.3 *In the* FIFE *model*

In an infinitesimal fluid element $d\mathcal{V} = dx\, dy\, dz$, the net outflow through the opposite surface sides of the fluid element in x-direction is $\frac{\partial(\rho V_x)}{\partial x} dx\, dy\, dz$, where V_x denotes the x-component

1 Historically, only the momentum equations were derived by Navier and Stokes. However, in computational fluid dynamics, the entire system of equations is often referred to as the Navier-Stokes equations nowadays.

of $\boldsymbol{V}$. Similar net flows are found in the y- and z-directions, giving a total outgoing net mass flow $\left(\frac{\partial(\rho V_x)}{\partial x}+\frac{\partial(\rho V_y)}{\partial y}+\frac{\partial(\rho V_z)}{\partial z}\right) dx\,dy\,dz$, which can be written as $\nabla\cdot(\rho\boldsymbol{V})$.

The net outgoing mass flow must equal the time rate of decrease of mass inside the element, $\frac{\partial\rho}{\partial t}dx\,dy\,dz$, and thus (after division by $dx\,dy\,dz$) in this model we find the equation

$$\frac{\partial\rho}{\partial t}+\nabla\cdot(\rho\boldsymbol{V})=0. \tag{3.5}$$

3.4.1.4 *In the* MIFE *model*

In the MIFE model, we follow a fluid element $\delta\mathscr{V}$ having a fixed mass. If we denote this mass by δm, then $\delta m=\rho\ \delta\mathscr{V}$, and since $\frac{D(\delta m)}{Dt}=0$,

$$0=\frac{D(\rho\ \delta\mathscr{V})}{Dt}=\rho\frac{D(\delta\mathscr{V})}{Dt}+\delta\mathscr{V}\frac{D\rho}{Dt},$$

or, remembering Equation 3.2:

$$\frac{D\rho}{Dt}+\rho\nabla\cdot\boldsymbol{V}=0. \tag{3.6}$$

3.4.1.5 *Relation between the equations*

Both finite control models give rise to equations that contain an integral, those are called *integral forms*. The infinitesimal fluid element models on the other hand, give rise to equations that are partially differential equations and are called the *partial differential equation forms*. Equations 3.3 and 3.5 are both in a form that emphasizes the principle of mass conservation and are therefore said to be in *conservation form*. The form of Equations 3.4 and 3.6 is called the *nonconservation form*.

It is easily seen that for instance Equations 3.3 and 3.5 are equivalent: the second integral in 3.3 can be rewritten to a volume integral using the divergence theorem. Taking the partial derivative inside the integral we find

$$\iiint_{\mathscr{V}}\frac{\partial\rho}{\partial t}+\nabla\cdot(\rho\boldsymbol{V})\,d\mathscr{V}=0.$$

Since this must hold for any arbitrary fixed volume $\mathscr{V}$, it must be that the integrand equals zero, which gives us Equation 3.5.

The equality of Equations 3.5 and 3.6 can be seen very easily by substituting $\nabla\cdot(\rho\boldsymbol{V})=\rho\nabla\cdot\boldsymbol{V}+\boldsymbol{V}\cdot(\nabla\rho)$ into 3.5 and applying the definition of the substantial derivative to 3.6.

For the proof of the other identities we refer to [1].

3.5 THE MOMENTUM EQUATION

Application of Newton's second law to one of the various flow models, gives a system of equations called the *momentum equation(s)*. In a viscid flow, the momentum equations become

quite complex, but when the flow is assumed to be inviscid, which for ocean modelling is a valid approximation, then the equations become a lot shorter. We will state the two differential forms. In Cartesian coordinates, write $\boldsymbol{V} = (v_x, v_y, v_z)^t$ and the equations are given by

$$\rho \frac{Dv_x}{Dt} = -\frac{\partial p}{\partial x} + \rho f_x, \tag{3.7a}$$

$$\rho \frac{Dv_y}{Dt} = -\frac{\partial p}{\partial y} + \rho f_y, \tag{3.7b}$$

$$\rho \frac{Dv_z}{Dt} = -\frac{\partial p}{\partial z} + \rho f_z, \tag{3.7c}$$

in *nonconservation form*, and equivalently in *conservation form* by

$$\frac{\partial(\rho v_x)}{\partial t} + \nabla \cdot (\rho v_x \boldsymbol{V}) = -\frac{\partial p}{\partial x} + \rho f_x, \tag{3.8a}$$

$$\frac{\partial(\rho v_y)}{\partial t} + \nabla \cdot (\rho v_y \boldsymbol{V}) = -\frac{\partial p}{\partial y} + \rho f_y, \tag{3.8b}$$

$$\frac{\partial(\rho v_z)}{\partial t} + \nabla \cdot (\rho v_z \boldsymbol{V}) = -\frac{\partial p}{\partial z} + \rho f_z. \tag{3.8c}$$

In those equations, p denotes the *pressure* and $\boldsymbol{f} = (f_x, f_y, f_z)^t$ is the body force (force acting on volumetric mass) per unit mass per volume. In viscous fluids, some extra terms appear due to normal and shear stress, which disappear in inviscid flows.

3.6 RELEVANT EQUATIONS

In Computational Fluid Dynamics, mainly the two partial differential equation-forms are used. For good measure, we restate these forms here.

Equation 3.6,

$$\frac{D\rho}{Dt} + \rho \nabla \cdot \boldsymbol{V} = 0, \tag{3.6}$$

from the MIFE-model is called a *nonconservation form*. Equation 3.5, from the FIFE-model,

$$\frac{\partial \rho}{\partial t} + \nabla \cdot (\rho \boldsymbol{V}) = 0, \tag{3.5}$$

is said to be in *conservation form*. When we assume the density ρ to be constant (as in an incompressible flow), those equations both are equivalent to

$$\boxed{\nabla \cdot \boldsymbol{V} = 0.} \tag{3.9}$$

From the momentum equations we will mostly use Equation 3.7, here given in vector notation:

$$\boxed{\rho \frac{D\boldsymbol{V}}{Dt} = -\nabla p + \rho \boldsymbol{f}.} \tag{3.10}$$

Another equation that may be of importance in Fluid Dynamics is the *energy equation*, based on the principle of energy conservation. However, for inviscid, incompressible, irrotational flows this equation follows from the momentum equation and it is superfluous. Therefore we left it out here.

3.7 STREAM FUNCTIONS

It would be good to mention here that when the vertical component of the flow velocity is assumed to be zero (which is a good approximation in a domain like ocean, we will come back to that later), so $\boldsymbol{V} = (v_x, v_y, 0)^t$, Equation 3.9 above implies $\frac{\partial v_x}{\partial x} = -\frac{\partial v_y}{\partial y}$, so if v_x is written as the derivative with respect to y of some scalar function $\psi(x,y,t)$, we find

$$v_x = \frac{\partial \psi}{\partial y}, \qquad v_y = -\frac{\partial \psi}{\partial x}. \tag{3.11}$$

Such a function ψ is called a *stream function*.

An important property of stream functions is that, when v_x and v_y are time independent at any point, and thus so is ψ, then since

$$\frac{d\psi}{dt} = \nabla\psi \cdot \boldsymbol{V} = \frac{\partial \psi}{\partial x}\frac{dx}{dt} + \frac{\partial \psi}{\partial y}\frac{dy}{dt} = \frac{\partial \psi}{\partial x}\frac{\partial \psi}{\partial y} - \frac{\partial \psi}{\partial y}\frac{\partial \psi}{\partial x} = 0,$$

a stream function is constant along all particle trajectories and we know that the gradient of ψ is perpendicular to its level curves.

3.8 PHYSICAL BOUNDARY CONDITIONS

Without imposing boundary conditions to the solution of a differential equation, it will in most cases not be unique. Though the conditions may be chosen differently for any model, common used conditions are that at the boundary walls of the domain either the total velocity, or the velocity component perpendicular to the wall, vanishes. These conditions imply that there is no slip along the boundary walls and that the boundary walls are non-porous, respectively. When B is the domain of *basin* under consideration, we can write these boundary conditions

$$\psi|_{\partial B} = 0, \qquad (\nabla\psi \cdot \boldsymbol{n})|_{\partial B} = 0, \tag{3.12}$$

which are the *Dirichlet* and *Neumann conditions*.

In the following chapter we will convert the equations from this chapter to a rotating spherical coordinate system and then give a more simple approximation to them that is applicable to a tangent plane.

4

GEOPHYSICAL FLUID DYNAMICS

In this chapter, the Navier-Stokes equations introduced earlier will be rewritten into spherical coordinates on a rotating spherical planet, such as the Earth. Due to the rotation, objects will experience a fictitious force or *pseudo force*. This effect is called the Coriolis effect, after the French scientist Gaspard-Gustave Coriolis, and is of main importance for the goal of this thesis. When the link between the fixed and rotating frames is studied, the Coriolis term will pop up automatically.

4.1 CORIOLIS FORCE

Consider two coordinate systems, both having an orthonormal sets of basis vectors with common origin, $\{\hat{\boldsymbol{x}}, \hat{\boldsymbol{y}}, \hat{\boldsymbol{z}}\}$ and $\{\hat{\boldsymbol{x}}', \hat{\boldsymbol{y}}', \hat{\boldsymbol{z}}'\}$ that rotate with respect to each other over time. We call the first coordinate system the *rotating system*, in which our planet would is fixed at the origin, and the second system is called the *fixed system*, in which the planet is rotating. We can set both z-axes to lie on the axis of rotation, such that

$$\hat{\boldsymbol{z}} \equiv \hat{\boldsymbol{z}}'. \tag{4.1}$$

The other two axes of the rotating system can than be defined as

$$\hat{\boldsymbol{x}} = \cos\Omega t\,\hat{\boldsymbol{x}}' + \sin\Omega t\,\hat{\boldsymbol{y}}' \tag{4.2}$$

and

$$\hat{\boldsymbol{y}} = -\sin\Omega t\,\hat{\boldsymbol{x}}' + \cos\Omega t\,\hat{\boldsymbol{y}}', \tag{4.3}$$

where Ω is the angular rotation frequency. For positive values of Ω, the direction of rotation agrees with Earth's rotational direction. Note that $\frac{d\hat{x}}{dt} = \Omega\hat{\boldsymbol{y}}$ and $\frac{d\hat{y}}{dt} = -\Omega\hat{\boldsymbol{x}}$, whereas $\frac{d\hat{z}}{dt} = 0$

Let $\boldsymbol{G} = G_1\hat{\boldsymbol{x}} + G_2\hat{\boldsymbol{y}} + G_3\hat{\boldsymbol{z}}$ be an arbitrary time-dependent vector function in the rotating basis. Then in the fixed basis, using time derivatives of the rotating frame vectors, the time derivative of $\boldsymbol{G}$ is

$$\begin{aligned}
\left[\frac{d\boldsymbol{G}}{dt}\right]_{\text{fxd}} &= \frac{dG_1}{dt}\hat{\boldsymbol{x}} + \frac{dG_2}{dt}\hat{\boldsymbol{y}} + \frac{dG_3}{dt}\hat{\boldsymbol{z}} + G_1\left[\frac{d\hat{\boldsymbol{x}}}{dt}\right]_{\text{fxd}} + G_2\left[\frac{d\hat{\boldsymbol{y}}}{dt}\right]_{\text{fxd}} + G_3\left[\frac{d\hat{\boldsymbol{z}}}{dt}\right]_{\text{fxd}} \\
&= \left[\frac{d\boldsymbol{G}}{dt}\right]_{\text{rot}} + \Omega\cdot(G_1\hat{\boldsymbol{y}} - G_2\hat{\boldsymbol{x}}) \\
&= \left[\frac{d\boldsymbol{G}}{dt}\right]_{\text{rot}} + \Omega\cdot(\hat{\boldsymbol{z}}\times\boldsymbol{G}),
\end{aligned}$$

where $\left[\frac{dG}{dt}\right]_{\text{rot}}$ is the time derivative of G with respect to the rotating frame, that is: the vectors $\hat{x}$, $\hat{y}$ and $\hat{z}$ are treated as constant vectors.

Let $\boldsymbol{\Omega} = \Omega\hat{z}$, then

$$\left[\frac{d\boldsymbol{G}}{dt}\right]_{\text{fxd}} = \left[\frac{d\boldsymbol{G}}{dt}\right]_{\text{rot}} + \boldsymbol{\Omega} \times \boldsymbol{G}. \tag{4.4}$$

In fact, the axis of rotation could be given by any fixed unit vector $\hat{v}$; then for angular frequency Ω we could define $\boldsymbol{\Omega} = \Omega\hat{v}$ and using this definition, Equation 4.4 would still hold.

For the second derivative we would find

$$\begin{aligned}\left[\frac{d^2\boldsymbol{G}}{dt^2}\right]_{\text{fxd}} &= \left[\frac{d^2\boldsymbol{G}}{dt^2}\right]_{\text{rot}} + \boldsymbol{\Omega} \times \left[\frac{d\boldsymbol{G}}{dt}\right]_{\text{rot}} + \boldsymbol{\Omega} \times \left[\frac{d\boldsymbol{G}}{dt}\right]_{\text{fxd}} \\ &= \left[\frac{d^2\boldsymbol{G}}{dt^2}\right]_{\text{rot}} + 2\boldsymbol{\Omega} \times \left[\frac{d\boldsymbol{G}}{dt}\right]_{\text{rot}} + \boldsymbol{\Omega} \times (\boldsymbol{\Omega} \times \boldsymbol{G}).\end{aligned}$$

When we consider $\boldsymbol{r}$ to be the trajectory of a fluid particle on a planet at the origin of the rotating system, and apply the above differentiation, we find

$$\left[\frac{d^2\boldsymbol{r}}{dt^2}\right]_{\text{fxd}} = \left[\frac{d^2\boldsymbol{r}}{dt^2}\right]_{\text{rot}} + 2\boldsymbol{\Omega} \times \left[\frac{d\boldsymbol{r}}{dt}\right]_{\text{rot}} + \boldsymbol{\Omega} \times (\boldsymbol{\Omega} \times \boldsymbol{r}). \tag{4.5}$$

The first term on the right-hand side, $\left[\frac{d^2\boldsymbol{r}}{dt^2}\right]_{\text{rot}}$, gives the acceleration with respect to the rotating frame. The second term, $2\boldsymbol{\Omega} \times \left[\frac{d\boldsymbol{r}}{dt}\right]_{\text{rot}}$, is called the *Coriolis force*. For matters of convenience we will write $\boldsymbol{v}_r = \left[\frac{d\boldsymbol{r}}{dt}\right]_{\text{rot}}$ from now on. The third term $\boldsymbol{\Omega} \times (\boldsymbol{\Omega} \times \boldsymbol{r})$ describes a *centripetal acceleration*, that on Earth induces a very small net force towards the equator. However, at Earth's surface, due to the low rotation speed, this term is so small that it is negligible:

$$\Omega \approx 7.2 \cdot 10^{-5} \text{ rad/s}, |\boldsymbol{r}| \approx 6.4 \cdot 10^{6} \text{ m} \implies |\boldsymbol{\Omega} \times (\boldsymbol{\Omega} \times \boldsymbol{r})| \leq \Omega^2 |\boldsymbol{r}| = 3.3 \cdot 10^{-2} \text{ m/s}^2,$$

which is a lot smaller than, for instance, gravity acceleration (9.8 m/s^2). Therefore, this term will be neglected and we will write

$$\left[\frac{d^2\boldsymbol{r}}{dt^2}\right]_{\text{fxd}} = \left[\frac{d\boldsymbol{v}_r}{dt}\right]_{\text{rot}} + 2\boldsymbol{\Omega} \times \boldsymbol{v}_r \tag{4.6}$$

onwards.

In small scale applications (such as water flow inside a pipeline or a river), the term $2\boldsymbol{\Omega} \times \boldsymbol{v}_r$ is also not relevant. In large scale applications like oceans however, it will not be negligible and it will be the goal of this thesis to describe its effect on the fluid dynamics at ocean level.

Recall that in the rotating frame we could define *spherical coordinates* as follows[1]:

$$\hat{\boldsymbol{r}} = \cos\theta\cos\phi\hat{\boldsymbol{x}} + \sin\theta\cos\phi\hat{\boldsymbol{y}} + \sin\phi\hat{\boldsymbol{z}}, \tag{4.7a}$$

$$\hat{\boldsymbol{\phi}} = -\cos\theta\sin\phi\hat{\boldsymbol{x}} - \sin\theta\sin\phi\hat{\boldsymbol{y}} + \cos\phi\hat{\boldsymbol{z}}, \tag{4.7b}$$

$$\hat{\boldsymbol{\theta}} = -\sin\theta\hat{\boldsymbol{x}} + \cos\theta\hat{\boldsymbol{y}}, \tag{4.7c}$$

which can be inverted to

$$\hat{\boldsymbol{x}} = \cos\theta\cos\phi\hat{\boldsymbol{r}} - \cos\theta\sin\phi\hat{\boldsymbol{\phi}} - \sin\theta\hat{\boldsymbol{\theta}}, \tag{4.8a}$$

$$\hat{\boldsymbol{y}} = \sin\theta\cos\phi\hat{\boldsymbol{r}} - \sin\theta\sin\phi\hat{\boldsymbol{\phi}} + \cos\theta\hat{\boldsymbol{\theta}}, \tag{4.8b}$$

$$\hat{\boldsymbol{z}} == \sin\phi\hat{\boldsymbol{r}} + \cos\phi\hat{\boldsymbol{\phi}}, \tag{4.8c}$$

such that

$$\boldsymbol{\Omega} = \Omega\left[\sin\phi\hat{\boldsymbol{r}} + \cos\phi\hat{\boldsymbol{\phi}}\right]. \tag{4.9}$$

The vector $\boldsymbol{v}_r := \left[\frac{d\boldsymbol{r}}{dt}\right]_{\text{rot}}$ may be written as

$$\boldsymbol{v}_r = v_r\hat{\boldsymbol{r}} + v_\phi\hat{\boldsymbol{\phi}} + v_\theta\hat{\boldsymbol{\theta}}, \tag{4.10}$$

where $v_r = \boldsymbol{v_r}\cdot\hat{\boldsymbol{r}} = r'$, $v_\phi = r\phi'$ and $v_\theta = r\theta'\cos\phi$, where the prime denotes a time derivative. We find[2]

$$\begin{aligned} 2\boldsymbol{\Omega}\times\boldsymbol{v_r} &= \Omega\left[\sin\phi\hat{\boldsymbol{r}} + \cos\phi\hat{\boldsymbol{\phi}}\right]\times\left[v_r\hat{\boldsymbol{r}} + v_\phi\hat{\boldsymbol{\phi}} + v_\theta\hat{\boldsymbol{\theta}}\right] \\ &= 2\Omega\left[\left(v_r\cos\phi - v_\phi\sin\phi\right)\hat{\boldsymbol{\theta}} + v_\theta\sin\phi\hat{\boldsymbol{\phi}} - v_\theta\cos\phi\hat{\boldsymbol{r}}\right]. \end{aligned} \tag{4.11}$$

We can find the time derivatives of the rotating unit vectors as follows: to find e.g. $\frac{d\hat{\boldsymbol{\theta}}}{dt}$, we differentiate 4.7c with respect to t to find

$$\begin{aligned} \frac{d\hat{\boldsymbol{\theta}}}{dt} &= -\theta'\cos\theta\hat{\boldsymbol{x}} - \theta'\sin\theta\hat{\boldsymbol{y}} \\ &= -\frac{v_\theta}{r\cos\phi}\left(\cos\theta\hat{\boldsymbol{x}} + \sin\theta\hat{\boldsymbol{y}}\right). \end{aligned}$$

Using the inverse of the basis vector transformations (Equations 4.8), we find

$$\frac{d\hat{\boldsymbol{\theta}}}{dt} = \frac{v_\theta}{r\cos\phi}\left(\sin\phi\hat{\boldsymbol{\phi}} - \cos\phi\hat{\boldsymbol{r}}\right). \tag{4.12a}$$

In similar fashion we find (see [4])

$$\frac{d\hat{\boldsymbol{\phi}}}{dt} = -\frac{v_\theta\tan\phi}{r}\hat{\boldsymbol{\theta}} - \frac{v_\phi}{r}\hat{\boldsymbol{r}} \tag{4.12b}$$

1 By convention, when a planet is considered in spherical coordinates, the angle ϕ denotes the latitude: at the equator, $\phi = 0°$, at the North Pole, $\phi = 90°$ and at the South Pole, $\phi = -90°$. The longitude is here denoted by θ and increases in eastward direction, where $\theta = 0°$ denotes some arbitrary prime meridian, here chosen such that it is contained in the $(y \geq 0, z)$-half-plane. The distance to the center of the planet is denoted by r. The unit vectors $\hat{\boldsymbol{\theta}}$, $\hat{\boldsymbol{\phi}}$ and $\hat{\boldsymbol{r}}$ denote the direction of an *infinitesimal increase* of θ, ϕ and r respectively.

2 The orthogonality relations in a spherical coordinate system (see [4, p. 268]): $\hat{\boldsymbol{\theta}}\times\hat{\boldsymbol{\phi}} = \hat{\boldsymbol{r}}$, $\hat{\boldsymbol{\phi}}\times\hat{\boldsymbol{r}} = \hat{\boldsymbol{\theta}}$ and $\hat{\boldsymbol{r}}\times\hat{\boldsymbol{\theta}} = \hat{\boldsymbol{\phi}}$.

and

$$\frac{d\hat{\boldsymbol{r}}}{dt} = \frac{v_\theta}{r}\hat{\boldsymbol{\theta}} + \frac{v_\phi}{r}\hat{\boldsymbol{\phi}}. \tag{4.12c}$$

Using these equalities we may calculate

$$\left[\frac{d\boldsymbol{v}_r}{dt}\right]_{\text{rot}} = \left(\frac{dv_\theta}{dt} - \frac{v_\theta v_\phi}{r}\tan\phi + \frac{v_\theta v_r}{r}\right)\hat{\boldsymbol{\theta}} + \left(\frac{dv_\phi}{dt} + \frac{v_\theta^2}{r}\tan\phi + \frac{v_\phi v_r}{r}\right)\hat{\boldsymbol{\phi}} + \left(\frac{dv_r}{dt} - \frac{v_\theta^2 + v_\phi^2}{r}\right)\hat{\boldsymbol{r}}. \tag{4.13}$$

Combining these last two gives

$$\left[\frac{d^2\boldsymbol{r}}{dt^2}\right]_{\text{fxd}} = \left(\frac{dv_\theta}{dt} - \frac{v_\theta v_\phi}{r}\tan\phi + \frac{v_\theta v_r}{r} + 2\Omega\left(v_r\cos\phi - v_\phi\sin\phi\right)\right)\hat{\boldsymbol{\theta}} + \left(\frac{dv_\phi}{dt} + \frac{v_\theta^2}{r}\tan\phi + \frac{v_\phi v_r}{r} + 2\Omega v_\theta\sin\phi\right)\hat{\boldsymbol{\phi}} + \left(\frac{dv_r}{dt} - \frac{v_\theta^2 + v_\phi^2}{r} - 2\Omega v_\theta\cos\phi\right)\hat{\boldsymbol{r}}. \tag{4.14}$$

The above equation is one of the main ingredients for the derivation of the geophysical fluid equations.

For a function f expressed in spherical coordinates, the *gradient* is given by (see [3, p. 221, Eqn. 8])

$$\nabla f = \frac{1}{r\cos\phi}\frac{\partial f}{\partial\theta}\hat{\boldsymbol{\theta}} + \frac{1}{r}\frac{\partial f}{\partial\phi}\hat{\boldsymbol{\phi}} + \frac{\partial f}{\partial r}\hat{\boldsymbol{r}}. \tag{4.15}$$

The conversion of a function from Cartesian to spherical coordinates is basic calculus.

The *divergence* of a vector function $\boldsymbol{G} = (G_\theta, G_\phi, G_r)^t$ is written in spherical coordinates as (see [3, p. 221, Eqn. 9][3])

$$\nabla\cdot\boldsymbol{G} = \frac{1}{r\cos\phi}\left(\frac{\partial G_\theta}{\partial\theta} + \frac{\partial(\cos\phi G_\phi)}{\partial\phi}\right) + \frac{\partial G_r}{\partial r} + \frac{2G_r}{r}. \tag{4.16}$$

4.2 THE NAVIER-STOKES EQUATIONS IN SPHERICAL COORDINATES

We observe that the substantial derivative of a vector equals as in Equation 3.10, can be written as

$$\frac{DV}{Dt} = \left[\frac{d^2\boldsymbol{r}}{dt^2}\right]_{\text{fxd}}, \tag{4.17}$$

3 Note that in [3] ϕ is defined to be zero at the North Pole, while in our discussion and in general in geophysics, $\phi = 0$ at the equator.

such that, taking the inner product of Equation 3.10 with $\hat{\boldsymbol{\theta}}$, $\hat{\boldsymbol{\phi}}$ and $\hat{\boldsymbol{r}}$, respectively, filling in the above and division by ρ, we find

$$\frac{dv_\theta}{dt} - \frac{v_\theta v_\phi}{r}\tan\phi + \frac{v_\theta v_r}{r} + 2\Omega\left(v_r\cos\phi - v_\phi\sin\phi\right) = -\frac{1}{\rho r\cos\phi}\frac{\partial p}{\partial\theta} + f_\theta, \tag{4.18a}$$

$$\frac{dv_\phi}{dt} + \frac{v_\theta^2}{r}\tan\phi + \frac{v_\phi v_r}{r} + 2\Omega v_\theta\sin\phi = -\frac{1}{\rho r}\frac{\partial p}{\partial\phi} + f_\phi, \tag{4.18b}$$

$$\frac{dv_r}{dt} - \frac{v_\theta^2 + v_\phi^2}{r} - 2\Omega v_\theta\cos\phi = -\frac{1}{\rho}\frac{\partial p}{\partial r} + f_r - g. \tag{4.18c}$$

From the continuity equation (Equation 3.9), we know, using Equation 4.16,

$$\frac{1}{r\cos\phi}\left(\frac{\partial v_\theta}{\partial\theta} + \frac{\partial(\cos\phi v_\phi)}{\partial\phi}\right) + \frac{\partial v_r}{\partial r} + \frac{2v_r}{r} = 0. \tag{4.19}$$

4.3 β-PLANE APPROXIMATION

When a flow is studied inside a small domain on the planet surface, it can be approximated by an *tangent plane*. If we fix a point $\boldsymbol{r}_0 = (\theta_0, \phi_0, r_0)^t$ in the rotating sperical coordinate system, we can define new[4] unit vectors $\hat{\boldsymbol{x}}, \hat{\boldsymbol{y}}, \hat{\boldsymbol{z}}$ around $\boldsymbol{r}_0$ that locally agree with

$$\hat{\boldsymbol{x}} = \hat{\boldsymbol{\theta}}, \qquad \hat{\boldsymbol{y}} = \hat{\boldsymbol{\phi}}, \qquad \hat{\boldsymbol{z}} = \hat{\boldsymbol{r}}, \tag{4.20}$$

such that by first order approximation we have a coordinate transformation for the coordinates x, y, z:

$$x = r_0\cos\phi_0\cdot(\theta - \theta_0), \qquad y = r_0(\phi - \phi_0), \qquad z = r - r_0. \tag{4.21}$$

We may calculate then

$$\frac{\partial}{\partial\theta} = r_0\cos\phi_0\frac{\partial}{\partial x}, \qquad \frac{\partial}{\partial\phi} = r_0\frac{\partial}{\partial y}, \qquad \frac{\partial}{\partial r} = \frac{\partial}{\partial z}. \tag{4.22}$$

This can be filled in into the equations of geophysical fluid dynamics in the previous section. The terms in the resulting equation that contain a factor $\frac{1}{r}$ are generally assumed to be negligible in addition to some other approximations, described in [11], resulting in the system of equations

$$\frac{Dv_x}{Dt} - fv_y = -\frac{1}{\rho}\frac{\partial p}{\partial x} + F_x, \tag{4.23a}$$

$$\frac{Dv_y}{Dt} + fv_x = -\frac{1}{\rho}\frac{\partial p}{\partial y} + F_y, \tag{4.23b}$$

$$\frac{Dv_z}{Dt} = -\frac{1}{\rho}\frac{\partial p}{\partial z} + F_z - g, \tag{4.23c}$$

4 These vectors have nothing to do with the unit vectors introduced earlier under the same names ($\hat{\boldsymbol{x}}$, $\hat{\boldsymbol{y}}$ and $\hat{\boldsymbol{z}}$). These names have only been chosen by regular convention.

where $f = 2\Omega\left(\sin\phi_0 + \frac{y}{r_0}\cos\phi_0\right)$ approximates $2\Omega\sin\phi$ around ϕ_0. When we take $\phi_0 = 0$, we find

$$\boxed{f = 2\Omega\frac{y}{r_0}.}$$

The continuity equation becomes just

$$0 = \frac{\partial v_x}{\partial x} + \frac{\partial v_y}{\partial y} + \frac{\partial v_z}{\partial z}. \tag{4.23d}$$

The dimensionless quantity $\frac{y}{r_0}$ is also called β, after which this approximation is called. When $\phi_0 = 0$, and also $y \ll r_0$, so close to the equator, the term $f(\beta)$ that represents the Coriolis force is negligible, as we would expect for horizontal movements at the equator[5].

Now we have derived the Navier-Stokes equations in a rotating spherical coordinate system, in the next chapter we will first make an approximation of fluid behaviour in shallow water in a non-rotating sytem and then add the Coriolis force to these equations.

5 At the equator, Coriolis force points radially inward toward the Earth's inner core.

5

SHALLOW WATER EQUATIONS

The goal of this chapter is to give a derivation of the *shallow water equations*, which describe the dynamics of flows in shallow water, that is, flows where the horizontal dimensions exceed the vertical dimensions largely, as is the case in oceans. We will mainly follow the lines of [4, ch. 8] to do so.

For simplicity, we will give the derivation for a two-dimensional basin. The equations are easily expanded to three-dimensional form.

5.1 DERIVATION OF THE EQUATIONS

Let b be a function of position x that describes the bottom height of the basin (also called the *bathymetry*), and h a function of position x and time t that describes the fluid height (or column) above the bottom surface. Assume the fluid to be homogeneous, such that ρ is constant in the time-dependent domain

$$B = \{(x,z) | b(x) < z < b(x) + h(x,t); x \in \mathbb{R}\}. \tag{5.1}$$

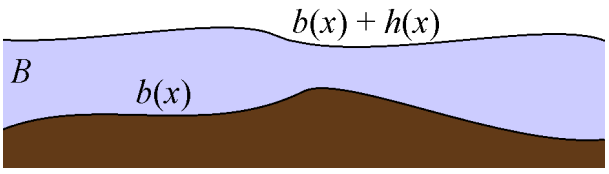

Figure 2.: *Sketch of a possible domain B, where the bathymetry (b) and water height (b + h) have been indicated.*

We denote the flow velocity by $\boldsymbol{V} = (v_x, v_z)^t$ and the Navier-Stokes equations give

$$\frac{\partial v_x}{\partial x} + \frac{\partial v_z}{\partial x} = 0 \tag{5.2a}$$

from the continuity equation (Equation 3.9), and

$$\frac{\partial v_x}{\partial t} + \boldsymbol{V} \cdot \nabla v_x = -\frac{1}{\rho}\frac{\partial p}{\partial x} + f_x, \tag{5.2b}$$

$$\frac{\partial v_z}{\partial t} + \boldsymbol{V} \cdot \nabla v_z = -\frac{1}{\rho}\frac{\partial p}{\partial z} - g + f_z \tag{5.2c}$$

from the momentum equations (in vector notation, Equation 3.10). We assume that both surfaces are *Lagrangian-invariant*, which means that fluid particles on the fluid remain on the fluid. For the bottom surface, this means it is impenetrable. On the top surface, a general assumption is that the pressure function is continuous over both sides of the surface.

For a particle trajectory on the bottom surface, we must have

$$z(t) = b(x(t)), \tag{5.3}$$

such that

$$\frac{dz}{dt}(t) = v_z(x, b(x), t) = v_x(x, b(x), t)\frac{\partial b}{\partial x}(x). \tag{5.4a}$$

Similarly, on the top surface, we find[1]

$$v_z(x, b+h, t) = \frac{\partial h}{\partial t}(x,t) + v_x(x, b+h, t)\left[\frac{\partial b}{\partial x}(x) + \frac{\partial h}{\partial x}(x,t)\right]. \tag{5.4b}$$

Equations 5.4 give the boundary conditions at the bottom (Equation 5.4a) and top (Equation 5.4b) boundaries of the domain B.

A first model can be derived by integration of Equation 5.2a over z from $b(x)$ to $b+h$, the entire water column:

$$\begin{aligned}\int_b^{b+h} \frac{\partial v_x}{\partial x}(x, \zeta, t)\, d\zeta &= -\int_b^{b+h} \frac{\partial v_z}{\partial z}(x, \zeta, t)\, d\zeta \\ &= -v_z(x, b+h, t) + v_z(x, b, t).\end{aligned} \tag{5.5}$$

By direct differentiation we know that

$$\begin{aligned}\frac{\partial}{\partial x}\left[\int_b^{b+h} v_x(x, \zeta, t)\, d\zeta\right] &= \int_b^{b+h} \frac{\partial v_x}{\partial x}(x, \zeta, t)\, d\zeta \\ &\quad - v_x(x, b+h, t)\left[\frac{\partial b}{\partial x}(x) + \frac{\partial h}{\partial x}(x,t)\right] + v_x(x, b, t)\frac{\partial b}{\partial x}(x).\end{aligned} \tag{5.6}$$

Combining this last equation with the boundary conditions (Equations 5.4), we can rewrite Equation 5.5 to

$$\frac{\partial}{\partial x}\left[\int_b^{b+h} v_x(x, \zeta, t)\, d\zeta\right] + \frac{\partial h}{\partial t}(x,t) = 0. \tag{5.7}$$

1 To save some space, we may write instead of $b(x)$ and $h(x,t)$ just b and h.

If we define $U(x,t)$ to be the average horizontal velocity in a fluid column,

$$U(x,t) = \frac{1}{h}\int_b^{b+h} v_x(x,\zeta,t)\, d\zeta, \tag{5.8}$$

we can rewrite Equation 5.7 to

$$\frac{\partial(hU)}{\partial x} + \frac{\partial h}{\partial t} = 0. \tag{5.9}$$

5.2 HYDROSTATIC APPROXIMATION

An approximation can be made into the governing system of equations by replacing Equation 5.2c by

$$0 = -\frac{1}{\rho}\frac{\partial p}{\partial z} - g. \tag{5.10}$$

This means that we neglect the vertical movement of fluid particles, and also the viscous dissipation, relative to the horizontal movement and the pressure gradient term. This method is sometimes called the *hydrostatic approximation*.

By integration of the above equation over the interval $(z, b+h)$, we find

$$p(x,z,t) = p_0 + \rho g \cdot (b+h-z), \tag{5.11}$$

where p_0 is the pressure at the ocean surface, which is assumed to be constant.

Differentiating the above, we can rewrite Equation 5.2b to

$$\frac{\partial v_x}{\partial t} + \boldsymbol{V}\cdot\nabla v_x = -g\left[\frac{\partial b}{\partial x}(x) + \frac{\partial h}{\partial x}(x,t)\right] + f_x \tag{5.12}$$

and using a same method of integration over the vertical water column (see [4, p. 295-296]), we arrive, together with Equation 5.9,

$$\frac{\partial(hU)}{\partial x} + \frac{\partial h}{\partial t} = 0, \tag{5.9, 5.13a}$$

at the equation below:

$$\frac{\partial(hU)}{\partial t} + \frac{\partial}{\partial x}\left[\int_b^{b+h} v_x^2\, d\zeta\right] = -g\left[\frac{\partial b}{\partial x}(x) + \frac{\partial h}{\partial x}(x,t)\right] h(x,t) + \int_b^{b+h} f_x\, d\zeta, \tag{5.13b}$$

which form the *system of shallow water equations*. When v_x does not depend on depth and neither does f_x, then $U \equiv v_x$ and Equations 5.13b become a lot simpler:

$$0 = \frac{\partial(hv_x)}{\partial x} + \frac{\partial h}{\partial t}, \tag{5.14a}$$

$$\frac{\partial(hv_x)}{\partial t} + \frac{\partial}{\partial x}\left[hv_x^2 + \frac{1}{2}gh^2\right] = -g\left[\frac{\partial b}{\partial x}(x)\right] h(x,t) + hf_x, \tag{5.14b}$$

which is called the *reduced* system of shallow water equations.

The shallow water equations can be extended to a three dimensional system trivially. Equation 5.14a, for instance, becomes

$$\nabla \cdot \left[h \begin{pmatrix} v_x \\ v_y \\ 0 \end{pmatrix} \right] + \frac{\partial h}{\partial t} = 0. \tag{5.15}$$

Equivalently we may write

$$\frac{Dh}{Dt} + h\left(\frac{\partial v_x}{\partial x} + \frac{\partial v_y}{\partial y}\right) = 0 \tag{5.16}$$

(note that h does not depend on z explicitly, such that the term $\frac{\partial h}{\partial z} v_z$ from $\frac{Dh}{Dt}$ vanishes).

5.3 CORIOLIS EFFECT ON THE SHALLOW WATER EQUATIONS

In the above derivation, we completely neglected the effect of Coriolis force on the equations.

We now add this force, by using the equations from the β-plane approximation (Equations 4.23), where for now we neglect all external forces except gravity. The equation for pressure becomes

$$p(x,y,z,t) = p_0 + \rho g[b(x,y) + h(x,y,t) - z],$$

such that the system of relevant equations becomes

$$\frac{Dv_x}{Dt} - f v_y = -g\left(\frac{\partial b}{\partial x} + \frac{\partial h}{\partial x}\right), \tag{5.17a}$$

$$\frac{Dv_y}{Dt} + f v_x = -g\left(\frac{\partial b}{\partial y} + \frac{\partial h}{\partial y}\right), \tag{5.17b}$$

$$\frac{Dh}{Dt} + h\left(\frac{\partial v_x}{\partial x} + \frac{\partial v_y}{\partial y}\right) = 0. \tag{5.17c}$$

5.4 THE MULTI-LAYER MODEL

So far, we assumed our ocean to be homogeneous. However, in fact the density of ocean water increases with depth. The model becomes more accurate if we account for this variation. This can be done by approximating the ocean by a multi-layer model: multiple layers that all have a different (constant) density. Equivalently, the density can be regarded as a step function.

We assume that layers with higher density lie below layers with lower density. Let $\rho_1 < \rho_2 < \ldots < \rho_n$ for some $n \in \mathbb{N}$ the possible values of the step function, then the domain becomes

$$B = B_1 \cup B_2 \cup \ldots \cup B_n, \tag{5.18}$$

where the B_i are the distinct layers having density ρ_i and B_{i+1} lies below B_i. We let h_i denote the height of the ith basin, and so B_1 lies between b and $b + h_1$, while B_2 lies between $b + h_1$

and $b+h_1+h_2$ and so on.

If we consider the two layer case of an inviscid flow two-dimensionally, so with no velocity component in y-direction, and let v_{ix} be the horizontal velocity in layer B_i, from Equation 5.14a we find

$$0 = \frac{\partial(h_1 v_{1x})}{\partial x} + \frac{\partial h_1}{\partial t}, \tag{5.19a}$$

$$0 = \frac{\partial(h_2 v_{2x})}{\partial x} + \frac{\partial h_2}{\partial t}, \tag{5.19b}$$

while from Equation 5.14b, we get

$$\frac{\partial(h_1 v_{1x})}{\partial t} + \frac{\partial}{\partial x}\left[h_1 v_{1x}^2 + \frac{1}{2} g h_1^2\right] = -g\left[\frac{\partial b}{\partial x}(x) + \frac{\partial h_2}{\partial x}(x,t)\right] h_1(x,t), \tag{5.19c}$$

$$\frac{\partial(h_2 v_{2x})}{\partial t} + \frac{\partial}{\partial x}\left[h_2 v_{2x}^2 + \frac{1}{2} g h_2^2\right] = -g\left[\frac{\partial b}{\partial x}(x) + \frac{\rho_1}{\rho_2}\frac{\partial h_1}{\partial x}(x,t)\right] h_2(x,t), \tag{5.19d}$$

as stated in [4].

5.5 LINEARIZATION OF THE SHALLOW WATER EQUATIONS

The differential equations we derived so far are nonlinear. The approach of this section is to derive linear differential equations from small perturbations to a simple solution of Equations 5.14 that has $v_x = 0$ and h equals some constant H, under the assumption that $b \equiv 0$ everywhere. The perturbed solution is written

$$(v_x(x,t), h(x,t)) = (0, H) + \varepsilon(\upsilon_x(x,t), \eta(x,t)), \tag{5.20}$$

where $0 < \varepsilon \ll 1$. We made the assumption here that v_x is independent from z.

Equation 5.14a can now be written as

$$0 = \varepsilon\frac{\partial \eta}{\partial t} + \varepsilon H\frac{\partial \upsilon_x}{\partial x} + \varepsilon^2\frac{\partial(\eta\upsilon_x)}{\partial x} = 0. \tag{5.21}$$

We divide the above by ε and assume ε to be small enough that the remaining ε-term can be ignored, giving the linear equation

$$\frac{\partial \eta}{\partial t} + H\frac{\partial \upsilon_x}{\partial x} = 0. \tag{5.22}$$

When the flow is considered to be inviscid, Equation 5.14b becomes in terms of the perturbation

$$\varepsilon H\frac{\partial \upsilon_x}{\partial t} + \varepsilon^2\frac{\partial(\eta\upsilon_x)}{\partial t} + \varepsilon^2 2\upsilon_x\frac{\partial \upsilon_x}{\partial x}\cdot(H+\varepsilon\eta) + \varepsilon^3\frac{\partial \eta}{\partial x}\upsilon_x^2 + g\cdot(H+\varepsilon\eta)\cdot\varepsilon\frac{\partial \eta}{\partial x} = 0. \tag{5.23}$$

If we ignore all terms that contain a factor ε^2 or ε^3, after division by εH, we arrive at the linear differential equation

$$\frac{\partial v_x}{\partial t} + g\frac{\partial \eta}{\partial x}, \tag{5.24}$$

such that the combination of the two linear differential equations gives two times the second order linear *wave equations*

$$0 = \frac{\partial^2 v_x}{\partial t^2} - gH\frac{\partial^2 v_x}{\partial x^2}, \tag{5.25}$$

$$0 = \frac{\partial^2 \eta}{\partial t^2} - gH\frac{\partial^2 \eta}{\partial x^2}. \tag{5.26}$$

Both equations above are of the same form,

$$\frac{\partial^2 u}{\partial t^2} - c^2\frac{\partial^2 u}{\partial x^2} = 0, \tag{5.27}$$

where $c = \sqrt{gH}$. In a basin of length L, a usual set of boundary (5.28) and initial (5.29) conditions is

$$u(0,t) = 0, \qquad u(L,t) = 0, \tag{5.28}$$

$$u(x,0) = f(x), \qquad \frac{\partial u}{\partial t}(x,0) = g(x). \tag{5.29}$$

We use the concepts of this chapter to solve some simple models in the following chapter, which will be used as a stepping stone to the discussion and solution of the Stommel model in Chapter 7.

6

SOME SIMPLE MODELS

Now we have derived and simplified all the relevant equations, we proceed by examining some simple models in this chapter to illustrate some techniques for solving them. The first model, of a *semi-infinite rectangular bay*, is quite similar to the Stommel model to be discussed in the next chapter, and is solved by using the technique of separation of variables. Also, a method will be given that solves models that are of the form of the *Poisson equation*.

6.1 SEMI-INFINITE RECTANGULAR BAY

The first simple model we will develop is of irrotational, incompressible flows in the region

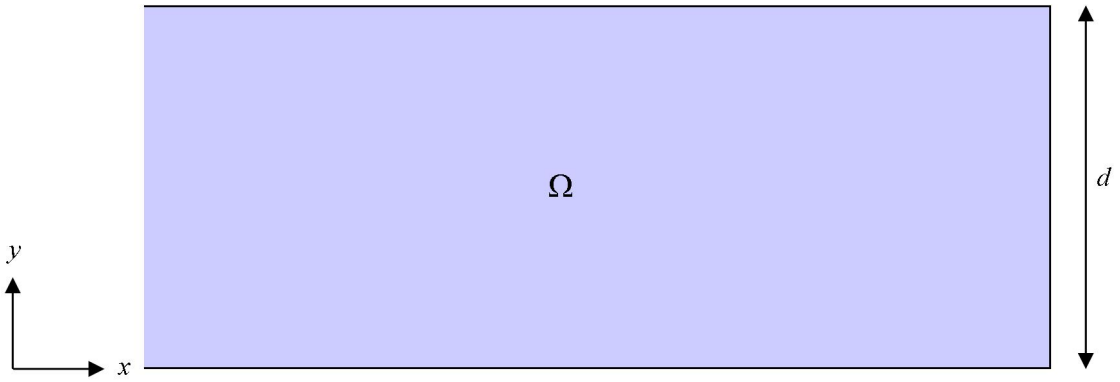

Figure 3.: *The bathymetry under consideration. It is semi-infinite towards the left (in negative $\hat{\mathbf{x}}$-direction).*

$$\Omega = \{(x,y)|x < 0; 0 < y < d\}, \tag{6.1}$$

which is the horizontal cross-section of a semi-infinite bay. As before, we assume the horizontal velocity not to depend on depth and for simplicity we ignore the vertical velocity entirely, such that our problem becomes a two-dimensional one in Ω. We also assume that both v_x and v_y do not change over time, that is, we are dealing with a *steady-state flow*. Therefore we know about the existence of a stream function ψ such that

$$v_x = \frac{\partial \psi}{\partial y}, \qquad v_y = -\frac{\partial \psi}{\partial x}. \tag{3.11}$$

Our goal is to find this function ψ.

Since the model is steady-state, $\frac{d\psi}{dt}$ will be zero and so any particle trajectory will be along a level curve of ψ, as described in Section 3.7. The flow is irrotational, so the curl of $\boldsymbol{V}$ is zero, meaning that

$$0 = \frac{\partial v_y}{\partial x} - \frac{\partial v_x}{\partial y} = -\frac{\partial^2 \psi}{\partial x^2} - \frac{\partial^2 \psi}{\partial y^2} = -\Delta\psi, \tag{6.2}$$

or simply $\Delta\psi = 0$.

When the seawalls are assumed to be impenetrable, we find boundary conditions

$$v_x(0,y) = 0 \text{ for } 0 < y < d, \tag{6.3}$$

$$\left.\begin{array}{l} v_y(x,0) = 0 \\ v_y(x,d) = 0 \end{array}\right\} \text{ for } x < 0. \tag{6.4}$$

In terms of ψ, we need that

$$\frac{\partial \psi}{\partial x}(x,0) = \frac{\partial \psi}{\partial x}(x,d) = \frac{\partial \psi}{\partial y}(0,y) = 0, \tag{6.5}$$

such that ψ is constant along the boundaries. By a continuity argument we assume that ψ has the same value along all three seawalls, and since adding a constant to ψ does not change its derivatives, we assume $\psi = 0$ along all boundaries:

$$\psi(x,y) = 0 \quad \forall (x,y) \in \partial\Omega. \tag{6.6}$$

This condition is called a *Dirichlet boundary condition*.

We use Fourier's method of separation of variables to find a solution. Suppose ψ can be written as

$$\psi(x,y) = F(x)G(y).$$

Then Equation 6.2 reduces to

$$\frac{F''(x)}{F(x)} + \frac{G''(y)}{G(y)} = 0 \text{ on } \Omega. \tag{6.7}$$

Since the first fraction depends solely on x and the second one on y, we conclude they must both be constant.

First assume $\frac{F''(x)}{F(x)} = \lambda^2 > 0$. Then

$$F''(x) - \lambda^2 F(x) = 0, \qquad G''(y) + \lambda^2 G(y) = 0, \tag{6.8}$$

giving

$$F(x) = a_1 e^{\lambda x} + a_2 e^{-\lambda x}, \qquad G(y) = b_1 \cos\lambda y + b_2 \sin\lambda y. \tag{6.9}$$

We can combine these functions to find

$$\psi(x,y) = \left[a_1 e^{\lambda x} + a_2 e^{-\lambda x}\right] \cdot \left[b_1 \cos\lambda y + b_2 \sin\lambda y\right]. \tag{6.10}$$

The condition $\psi(x,0) = 0$ gives either $a_1 = a_2 = 0$ or $b_1 = 0$. We choose the latter since the former represents the trivial solution $\psi(x,y) = 0$ for all $(x,y) \in \Omega$, and we can write now

$$\psi(x,y) = \left[Ae^{\lambda x} + Be^{-\lambda x}\right] \cdot \sin \lambda y \tag{6.11}$$

by defining $A = a_1 b_2$ and $B = a_2 b_2$.

The second condition, $\psi(0,y) = 0$, gives as non-trivial solution $(A+B) = 0$, or $A = -B$, such that ψ becomes

$$\psi(x,y) = C \sinh \lambda x \cdot \sin \lambda y, \tag{6.12}$$

where $C = 2A$.

The last step is to apply the condition $\psi(x,d) = 0$, giving either $C = 0$ or $\sin \lambda d = 0$. The latter expression is the non-trivial one, giving $\lambda d = n\pi$ ($n \in \mathbb{Z}$), or

$$\lambda_n = \frac{n\pi}{d}, \quad n \in \mathbb{Z}. \tag{6.13}$$

Since sin and sinh are both odd functions, their product is even and thus λ_n and λ_{-n} give the same result. Furthermore, λ_0 gives the trivial solution $\psi = 0$, so we only need to consider $n \in \mathbb{N}$, giving the linearly independent solutions

$$\psi_n(x,y) = C_n \sinh \frac{n\pi x}{d} \sin \frac{n\pi y}{d}. \tag{6.14}$$

It is easily seen that any linear combination of solutions of the above form is also a solution. Therefore, we can impose another boundary condition, for instance at the line $x = s$, by requiring

$$\psi(s,y) = f(y).$$

Using the theory of Fourier series, we can now find C_n as

$$C_n = \frac{2}{d \sinh \frac{n\pi a}{d}} \int_0^d f(y) \sin \frac{n\pi y}{d} \, dy. \tag{6.15}$$

When we assume $\frac{F''(x)}{F(x)} = -\lambda^2 < 0$, then we would get the solution functions

$$\psi(x,y) = [a_1 \cos \lambda x + a_2 \sin \lambda x] \cdot \left[b_1 e^{\lambda y} + b_2 e^{-\lambda y}\right]. \tag{6.16}$$

However, using the same procedure as for the positive case, we first apply $\psi(0,y) = 0$ to find $a_1 = 0$, then we observe that $\psi(x,0) = 0$ requires $b_1 = -b_2$ so ψ is of the form

$$\psi(x,y) = C \sin \lambda x \cdot \sinh \lambda y.$$

But then $\psi(x,d) = 0$ implies[1] $C = 0$ so this way we only find the trivial solution $\psi(x,y) = 0$.

1 Since $\sinh \lambda d = 0$ iff $\lambda = 0$ and $\lambda^2 > 0$, so $\lambda \neq 0$.

6.2 EIGENFUNCTIONS OF THE LAPLACE OPERATOR

When for some operator F, the equation $F(\psi) = \mu\psi$ has non-trivial solutions (μ_i, ψ_i), the scalar constant μ_i is called an eigenvalue and the corresponding function ψ_i is called an eigenfunction of the operator F. In this section we present the eigenfuntions of the Laplace operator Δ.

On the domain

$$\Omega = \{(x,y)|0 < x < a; 0 < y < b\}, \tag{6.17}$$

the *Laplace operator* Δ has eigenfunctions ψ corresponding to eigenvalues $-\lambda_{nm}^2$, satisfying the boundary condition

$$\psi_{nm}(x,y) = 0 \quad \forall (x,y) \in \partial\Omega,$$

which are of the form

$$\psi_{nm}(x,y) = A_{nm} \sin\frac{n\pi x}{a} \sin\frac{m\pi y}{b}, \tag{6.18}$$

where

$$\lambda_{nm}^2 = \left(\frac{n^2}{a^2} + \frac{m^2}{b^2}\right)\pi^2, \quad n,m \in \mathbb{N}. \tag{6.19}$$

6.3 POISSION EQUATION SOLUTIONS

We can use the above to approximate solutions of the general *Poisson equation*

$$\Delta\psi = -f(x,y); \quad \psi = 0 \text{ on } \partial\Omega. \tag{6.20}$$

First we can approximate f by a linear combination of the functions ψ_{nm}, using the techniques known from any Linear Algebra course:

$$f(x,y) = \sum_{n,m}^{\infty} A_{nm} \sin\frac{n\pi x}{a} \sin\frac{m\pi y}{b}, \tag{6.21}$$

where

$$A_{nm} = \frac{4}{ab}\int_0^a \int_0^b f(x,y) \sin\frac{n\pi x}{a} \sin\frac{m\pi y}{b}\, dx\, dy. \tag{6.22}$$

We also want to express ψ in terms of the ψ_{nm}

$$\psi(x,y) = \sum_{n,m}^{\infty} B_{nm} \sin\frac{n\pi x}{a} \sin\frac{m\pi y}{b}.5 \tag{6.23}$$

Our problem is to find the coefficients B_{mn}.

Since the Laplacian Δ is a *linear* operator,

$$\begin{aligned} \Delta\psi &= \sum_{n,m}^{\infty} \Delta\left(B_{nm} \sin\frac{n\pi x}{a} \sin\frac{m\pi y}{b}\right) \\ &= \sum_{n,m}^{\infty} -\lambda_{nm}^2 \left(B_{nm} \sin\frac{n\pi x}{a} \sin\frac{m\pi y}{b}\right), \end{aligned} \tag{6.24}$$

such that we need $\lambda_{nm}^2 B_{nm} = A_{nm}$, or

$$B_{nm} = \frac{A_{nm}}{\lambda_{nm}^2}.$$

Now we have solved some simple models, in the next chapter we proceed to solving the Stommel model which is a bit more complicated.

7

THE STOMMEL MODEL

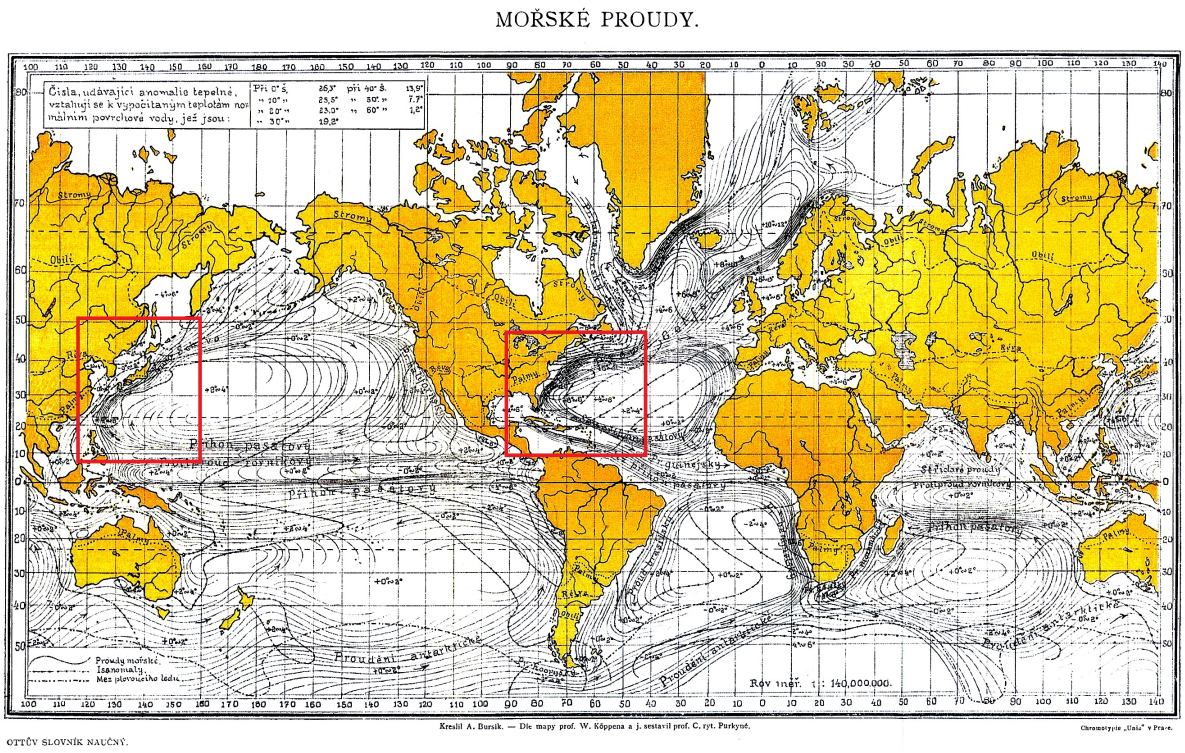

Figure 4.: *Picture by Cyrill Purkyně and A. Bursík, taken from [7], showing ocean streamlines. The red boxes (drawn by the author) indicate regions around the western border of an ocean stream, where clearly the streamlines are more dense than at the eastern parts of the streams. The Gulf Stream is situated between Europe/Northwest Africa and North America.*

In this chapter we will discuss the Stommel model, which was first introduced by Henry Stommel in his paper, [10], called "The Westward Intensification Of Wind-Driven Ocean Currents", published in 1948, and which is also discussed in [4, sec. 9]. It is a simple model of ocean circulation that takes into account the most prominent forces that affect the flow of the fluid particles in ocean streams like the Gulf Stream.

The goal of Stommel's paper, which was published in a scientific geophysical magazine, was to give an explanation for the relatively high intensity of streamlines around the western borders of oceans, seen for example in Figure 4. It was not necessarily his intention to give a model

that accurately describes the fluid flows, but to produce a very simple model that still shows accordance to reality at the level of these streamlines.

7.1 EQUATIONS AND APPROXIMATIONS

In his work, Stommel considers a rectangular basin with ground plane

$$\{(x,y)|0<x<\lambda;0<y<b\}$$

and a time-independent height $D+h(x,y)$, where D is the constant water height when the water is at rest. Due to currents, the water height will slightly deviate from D, by an amount of h, so the interface between sea and air is at $z=D+h$. Stommel assumes the water to be homogeneous and incompressible, such that the density, $\rho=\rho_0$, is constant. Furthermore he ignores all vertical movement.

On the northern hemisphere, the sea wind at small latitudes is towards the (south-)western direction and at higher latitudes in (north-)eastern direction. For simplicity, Stommel ignores the wind components in north-south direction and simplifies the wind stress $\boldsymbol{T}$ on the water surface to be

$$\boldsymbol{T}(y)=\begin{pmatrix}-T\cos\frac{\pi y}{b}\\0\\0\end{pmatrix}, \tag{7.1}$$

in agreement with the directions on the northern hemisphere (T is some constant).

In order to prevent the water in the model from accelerating to infinite speeds, Stommel also adds a bottom friction term $\boldsymbol{R}$:

$$\boldsymbol{R}=-R\boldsymbol{V}=-R\begin{pmatrix}v_x\\v_y\\0\end{pmatrix}, \tag{7.2}$$

where $\boldsymbol{V}=(v_x,v_y,0)$ is the velocity vector and R is some constant. How exactly these terms appear in the equations, will become clear further below.

We apply these concepts to the equations from the β-plane approximation (Equations 4.23) and assume that the $\frac{D\boldsymbol{V}}{Dt}$-terms are negligible compared to the other factors[1], as Stommel did.

These equations then become

$$-\rho_0 f v_y=-\frac{\partial p}{\partial x}+\rho_0 F_x, \tag{7.3a}$$

$$\rho_0 f v_x=-\frac{\partial p}{\partial y}+\rho_0 F_y, \tag{7.3b}$$

$$0=-\frac{\partial p}{\partial z}+\rho_0 F_z, \tag{7.3c}$$

1 In doing so, we neglect the nonlinear term $\boldsymbol{V}\cdot\nabla\boldsymbol{V}$ and arrive at a linear differential equation. The non-linear case where this term is not being neglected, will be given at the end of Chapter 8.

and

$$0 = \frac{\partial v_x}{\partial x} + \frac{\partial v_y}{\partial y}. \tag{7.3d}$$

where $F_z = -g$, while F_x and F_y are related to $\boldsymbol{R}$ and $\boldsymbol{T}$.

Integration of Equation 7.3d with respect to z gives

$$p(x,y,z,t) = p_0 + \int_z^{D+h} -\rho_0 g = p_0 + \rho_0 g \cdot [D + h(x,y,t) - z], \tag{7.4}$$

where the air pressure p_0 is assumed to be constant with respect to time and position, as in [4].

Substituting this into Equations 7.3a and 7.3b gives, after division by ρ_0,

$$-f v_y = -g\frac{\partial h}{\partial x} + F_x, \tag{7.5a}$$

$$f v_x = -g\frac{\partial h}{\partial y} + F_y. \tag{7.5b}$$

If we integrate the above equations from $z = 0$ to $z = D + h$, which is an easy calculation since the terms in the equations do not depend on z, and make the approximation $D \approx D + h$, we find that

$$-f v_y D = -g\frac{\partial h}{\partial x} D + F_x D, \tag{7.6a}$$

$$f v_x D = -g\frac{\partial h}{\partial y} D + F_y D. \tag{7.6b}$$

Here Stommel lets $F_x D$ equal the x-component of $\boldsymbol{T} + \boldsymbol{R}$ and $F_y D$ its y-component.

Looking at Equation 7.3d, we recall from Section 3.7 that we can use a stream function ψ to express the components of $\boldsymbol{V}$: we can write $v_x = \frac{\partial \psi}{\partial y}$ and $v_y = -\frac{\partial \psi}{\partial x}$. When we do this and apply this to the right partial derivatives of Equations 7.6, we find

$$\overbrace{-\frac{\partial f}{\partial y}\frac{\partial \psi}{\partial x}}^{\frac{\partial f}{\partial y}\frac{\partial \psi}{\partial x}} \underbrace{-f\frac{\partial v_y}{\partial y} - f\frac{\partial v_x}{\partial x}}_{-f\cdot\left(\frac{\partial v_x}{\partial x}+\frac{\partial v_y}{\partial y}\right)=0} = \overbrace{\frac{R}{D}\frac{\partial v_y}{\partial x} - \frac{R}{D}\frac{\partial v_x}{\partial y}}^{-\frac{R}{D}\Delta\psi} + \frac{T\pi}{Db}\sin\frac{\pi y}{b}, \tag{7.7}$$

such that we arrive at the partial differential equation that does not depend on time explicitly:

$$\Delta\psi + \alpha\frac{\partial \psi}{\partial x} = \gamma \sin\frac{\pi y}{b}, \tag{7.8}$$

where

$$\alpha = \frac{D}{R}\frac{\partial f}{\partial y}, \qquad \gamma = \frac{T\pi}{Rb}. \tag{7.9}$$

The boundary condition applied by Stommel is just the condition we also introduced in the previous chapter, namely that ψ is zero at the boundary of the basin:

$$\psi(0,y,t) = \psi(\lambda,y,t) = \psi(x,0,t) = \psi(x,b,t) = 0 \text{ for all } x,y,t. \tag{7.10}$$

Typical values for the constants in [4] and [10] are

$$D = 2 \cdot 10^2 \text{ m}, \qquad \lambda = 10^7 \text{ m}, \qquad b = 2\pi \cdot 10^6 \text{ m},$$

while the wind and bottom friction parameters T and R are given the values

$$T = 0.1 \text{ m}^2/\text{s}^2, \qquad R = 0.02 \text{ m/s}$$

in order to make the results comparable to reality[2].

The value of α is given by $\alpha = \frac{D}{R}\frac{\partial f}{\partial y}$. Up to first order around the equator (at $y = 0$), $f(y) = 2\Omega\frac{y}{r_0}$, where $\Omega = \frac{2\pi}{60 \cdot 60 \cdot 24}$ s^{-1} and $r_e = 6.24 \cdot 10^6$ m are the angular frequency and radius of the earth. For small y-values we thus find $\frac{\partial f}{\partial y} \approx 2 \cdot 10^{-11}$ m^{-1}s^{-1} and for simplicity we approximate $\frac{\partial f}{\partial y}$ to be equal to this value constantly.

7.2 THE STREAM FUNCTION

The differential equation 7.8 has, as Stommel states, a particular solution

$$\psi_p(x,y) = -\gamma\frac{b^2}{\pi^2}\sin\frac{\pi y}{b}, \tag{7.11}$$

while the homogeneous equation is

$$\Delta\psi_h + \alpha\frac{\partial\psi_h}{\partial x} = 0. \tag{7.12}$$

Using the method of separation of variables, by writing $\psi_h(x,y) = F(x)G(y)$, in which the differential equation reduces to

$$F''(x)G(y) + F(x)G''(y) + \alpha F'(x)G(y) = 0, \tag{7.13}$$

or

$$\frac{F''(x) + \alpha F'(x)}{F(x)} = -\frac{G''(y)}{G(y)}, \tag{7.14}$$

where both fractions must be constant as before. In the case where $\frac{F''(x)+\alpha F'(x)}{F(x)} = -\frac{G''(y)}{G(y)} = -\beta^2 < 0$, we find $G(y) = b_1 e^{\beta y} + b_2 e^{-betay}$. Applying the boundary conditions $\psi_p(x,0) = \psi_p(x,b) = 0$, we find either the trivial solution $F(x) = 0$ or the conditions $G(0) = G(b) = 0$.

2 This value of T corresponds to a force per unit area of $\rho_0 T \approx 100$ N/m^2.

The first one, $G(0) = 0$, implies $b_1 = -b_2$, while the second one implies $b_1 = -b_2 e^{-2\beta b}$. Since $\beta \neq 0$ and $b > 0$, this also leads to the trivial solution. Therefore we assume

$$\frac{F''(x) + \alpha F'(x)}{F(x)} = -\frac{G''(y)}{G(y)} = \beta^2 > 0,$$

such that we have solutions for $G''(y) + \beta^2 G(y) = 0$:

$$G(y) = b_1 \sin \beta y + b_2 \cos \beta y, \tag{7.15}$$

where b_1 and b_2 are arbitrary constants. We know $\psi_p(x,0) = \psi_p(x,b) = 0$, such that the condition $\psi(x,0) = \psi(x,b) = 0$ implies that ψ_h is zero at $y = 0$ and $y = b$. This either gives $F(x) = 0$, the trivial solution, or $G(0) = G(b) = 0$, which is the property we will assume to find a non-trivial solution. Since $G(0) = 0$, we need $b_2 = 0$, and thus

$$G(y) = b_1 \sin \beta y. \tag{7.15*}$$

The condition $G(b) = 0$ gives $\beta b = k\pi$ with $k \in \mathbb{N}$ (or in $\mathbb{Z}$, but a negative k only adds a minus sign, which can also be caught into b_1), such that we find possibilities $\beta_k = \frac{k\pi}{b}$.

The second differential equation we need to solve is

$$F''(x) + \alpha F'(x) - \beta^2 F(x) = 0.$$

A well-known method from differential calculus to solve this equation is to suggest a solution $F(x) = e^{\mu x}$. Applying this suggestion, gives

$$(\mu^2 + \alpha\mu - \beta^2) e^{\mu x} = 0,$$

which we can solve for μ:

$$\mu = \frac{-\alpha \pm \sqrt{\alpha^2 + 4\beta^2}}{2}. \tag{7.16}$$

This gives, by linear combination of the $+$ and $-$-solutions, the general solution

$$F(x) = e^{-\frac{\alpha}{2}x} \left(a_1 \sinh \kappa x + a_2 \cosh \kappa x \right), \tag{7.17}$$

where $\kappa = \sqrt{\frac{\alpha^2}{4} + \beta^2}$.

We can now write

$$\psi_{h,k}(x,y) = e^{-\frac{\alpha}{2}x} \sin(\beta_k y) \left(A_k \sinh \kappa_k x + B_k \cosh \kappa_k x \right), \tag{7.18}$$

where $A_k = a_1 b_1$ and $B_k = a_2 b_1$ are the appropriate constants, giving a full solution

$$\psi(x,y) = e^{-\frac{\alpha}{2}x} \sum_{k=1}^{\infty} \left[\sin(\beta_k y) \left(A_k \sinh \kappa_k x + B_k \cosh \kappa_k x \right) \right] - \gamma \frac{b^2}{\pi^2} \sin \frac{\pi y}{b}. \tag{7.19}$$

The condition $\psi(0,y)=0$ implies

$$\sum_{k=1}^{\infty}\left[\sin(\beta_k y)B_k\right]-\gamma\frac{b^2}{\pi^2}\sin\frac{\pi y}{b}=0$$

for all y, giving $B_1=\gamma\frac{b^2}{\pi^2}$, and $B_i=0$ for $i>1$.

The final condition, $\psi(\lambda,y)=0$, tells us

$$\sum_{k=1}^{\infty}e^{-\frac{\alpha}{2}\lambda}\left[A_k\sin(\beta_k y)\sinh\kappa_k\lambda\right]-\gamma\frac{b^2}{\pi^2}\sin\frac{\pi y}{b}\left(1-e^{-\frac{\alpha}{2}\lambda}\cosh\kappa_1\lambda\right)=0.$$

We solve this for A_k by first letting $A'_k=A_k e^{-\frac{\alpha}{2}\lambda}\sinh\kappa_k\lambda$ and solving

$$\sum_{k=1}^{\infty}A'_k\sin\frac{k\pi y}{b}=\gamma\frac{b^2}{\pi^2}\sin\frac{\pi y}{b}\left(1-e^{-\frac{\alpha}{2}\lambda}\cosh\kappa_1\lambda\right),$$

which gives

$$\begin{aligned}A'_k&=\frac{2}{b}\gamma\frac{b^2}{\pi^2}\left(1-e^{-\frac{\alpha}{2}\lambda}\cosh\kappa_1\lambda\right)\int_0^b\sin\frac{\pi y}{b}\sin\frac{k\pi y}{b}\,dy\\&=\begin{cases}\gamma\frac{b^2}{\pi^2}\left(1-e^{-\frac{\alpha}{2}\lambda}\cosh\kappa_1\lambda\right) & \text{if } k=1\\ 0 & \text{if } k\neq 1\end{cases},\end{aligned}\tag{7.20}$$

such that $A_1=\gamma\frac{b^2}{\pi^2}\frac{1-e^{-\frac{\alpha}{2}\lambda}\cosh\kappa_1\lambda}{e^{-\frac{\alpha}{2}\lambda}\sinh\kappa_1\lambda}=\gamma\frac{b^2}{\pi^2}\frac{e^{\frac{\alpha}{2}\lambda}-\cosh\kappa_1\lambda}{\sinh\kappa_1\lambda}$.

The full solution now becomes

$$\psi(x,y)=\gamma\frac{b^2}{\pi^2}e^{-\frac{\alpha}{2}x}\sin\frac{\pi y}{b}\left(\frac{e^{\frac{\alpha}{2}\lambda}-\cosh\kappa\lambda}{\sinh\kappa\lambda}\sinh\kappa x+\cosh\kappa x-e^{\frac{\alpha}{2}x}\right),\tag{7.21}$$

with $\kappa=\sqrt{\frac{\alpha^2}{4}+\frac{\pi^2}{b^2}}$.

7.3 THE WATER HEIGHT

From the stream function ψ in Equation 7.21 we can find by differentiation

$$v_x(x,y)=\frac{\partial\psi}{\partial y}=\gamma\frac{b}{\pi}e^{-\frac{\alpha}{2}x}\cos\frac{\pi y}{b}\left(\frac{e^{\frac{\alpha}{2}\lambda}-\cosh\kappa\lambda}{\sinh\kappa\lambda}\sinh\kappa x+\cosh\kappa x-e^{\frac{\alpha}{2}x}\right),$$

$$\begin{aligned}v_y(x,y)=-\frac{\partial\psi}{\partial x}=-\gamma\frac{b^2}{\pi^2}e^{-\frac{\alpha}{2}x}\sin\frac{\pi y}{b}\Bigg[&-\frac{\alpha}{2}\left(\frac{e^{\frac{\alpha}{2}\lambda}-\cosh\kappa\lambda}{\sinh\kappa\lambda}\sinh\kappa x+\cosh\kappa x\right)\\&+\kappa\left(\frac{e^{\frac{\alpha}{2}\lambda}-\cosh\kappa\lambda}{\sinh\kappa\lambda}\cosh\kappa x+\sinh\kappa x\right)\Bigg].\end{aligned}$$

such that we can solve the equations 7.6 to find h up to a constant. Using the linear approximation $f(y) \approx \frac{\alpha R}{D} y$ and rewriting Equation 7.6b, we find

$$\begin{aligned}\frac{\partial h}{\partial y} &= \frac{-f(y)v_x(x,y) - R/D \cdot v_y(x,y)}{g} \\ &= K_1(x) y \cos\frac{\pi y}{b} + K_2(x)\sin\frac{\pi y}{b},\end{aligned}$$

where K_1 and K_2 are functions of x that contain all constant factors and factors depending on x that appear in $\frac{\partial h}{\partial y}$, which for matters of convenience we do not write down explicitly here. Integration and substitution of K_1 and K_2 gives

$$\begin{aligned}h(x,y) = C(x) - \frac{b^2}{\pi^2}\frac{T\alpha}{gD} e^{-\frac{\alpha}{2}x}\Bigg[&\frac{\pi y}{b}\sin\frac{\pi y}{b}\cdot\left(B\sinh\kappa x + \cosh\kappa x - e^{\frac{\alpha}{2}x}\right) \\ &+ \cos\frac{\pi y}{b}\cdot\left(\frac{1}{2}\left(B\sinh\kappa x + \cosh\kappa x\right) + \frac{\kappa}{\alpha}\left(B\cosh\kappa x + \sinh\kappa x\right) - e^{\frac{\alpha}{2}x}\right)\Bigg],\end{aligned} \tag{7.22}$$

where $B = \frac{e^{\frac{\alpha}{2}\lambda} - \cosh\kappa\lambda}{\sinh\kappa\lambda}$. Taking the derivative of the above with respect to x and comparing to Equation 7.6a, tells us $\frac{\partial C(x)}{\partial x} = 0$, so C is an arbitrary constant and we put it equal to zero, giving

$$\begin{aligned}h(x,y) = -\frac{b^2}{\pi^2}\frac{T\alpha}{gD} e^{-\frac{\alpha}{2}x}\Bigg[&\frac{\pi y}{b}\sin\frac{\pi y}{b}\cdot\left(B\sinh\kappa x + \cosh\kappa x - e^{\frac{\alpha}{2}x}\right) \\ &+ \cos\frac{\pi y}{b}\cdot\left(\frac{1}{2}\left(B\sinh\kappa x + \cosh\kappa x\right) + \frac{\kappa}{\alpha}\left(B\cosh\kappa x + \sinh\kappa x\right) - e^{\frac{\alpha}{2}x}\right)\Bigg].\end{aligned} \tag{7.22*}$$

7.4 VORTICITY

Vorticity is a pseudovector field describing the local spinning motion of the flow and is defined as $\boldsymbol{\omega} = \nabla \times \boldsymbol{V}$. In the case that $\boldsymbol{V} = (\psi_y(x,y), -\psi_x(x,y), 0)^t$, the x- and y-components of $\boldsymbol{\omega}$ are both zero and the z-component equals

$$\begin{aligned}\omega_z &= \frac{\partial}{\partial x}v_y - \frac{\partial}{\partial y}v_x \\ &= -\psi_{xx} - \psi_{yy} \\ &= -\Delta\psi.\end{aligned} \tag{7.23}$$

A negative value of ω_z implies that the spin is locally in clockwise direction when observing the sea from above. Straightforward calculation gives

$$\omega_z = -\gamma\sin\frac{\pi y}{b}\left(1 + \frac{b^2}{\pi^2}e^{-\frac{\alpha}{2}x}\left[\frac{\alpha^2}{2}\left(B\sinh\kappa x + \cosh\kappa x\right) - \alpha\kappa\left(B\cosh\kappa x + \sinh\kappa x\right)\right]\right). \tag{7.24}$$

There are several conclusions that we may draw from Equations 7.21, 7.22* and 7.24. A first observation is that in both ψ and h the wind stress coefficient T has been factored out into a multiplicative constant (remember that $\gamma = \frac{T\pi}{Rb}$), such that a change in T would not change the shape of the streamlines and the surface contours, except when $T = 0$. For $T = 0$, of course, the stable solution without rotation is a stationary ocean where h is constant. In that case, the Coriolis force would by its velocity dependence be equal to zero and so when the planet's rotation is considered, the result would still be a non-rotating ocean.

Another observation is the appearance of the term $e^{-\frac{\alpha}{2}x}$ in both formulas. As mentioned before, the goal of Stommel's model is to explain the intensification of stream curves in westward direction. This intensification is due to this exponential term only: By definition, $\alpha \propto \Omega$, so $\Omega = 0$ implies that $\alpha = 0$. When $\Omega = 0$, the term $e^{-\frac{\alpha}{2}x}$ is constant and both ψ and h are symmetric under rotation over 180° around the center of the basin, as can be seen from Figure 5. Remember that in the southern half of the basin, the wind is in westward direction, and in the northern half it blows eastward. This causes the water level to be pushed towards the southwest and northeast corners.

When Ω is increased, $e^{-\frac{\alpha}{2}x}$ becomes non-constant and ψ and h are both flattened out in eastward direction, pulling all streamlines westward, giving the effect Stommel wanted to model. In Figure 6, we see the contour and surface plots of ψ and h when Ω equals the Earth's rotational frequency. In Figure 7, the value of Ω is again increased to twice Earth's rotational frequency, and one observes an even greater westwards stretch of the contour lines.

When the model is applied to a basin at the southern hemisphere instead, α will remain the same so, as Stommel states in [10], the crowding of streamlines is still toward the western ocean border.

In all cases the circulation is in clockwise direction, as is indicated by the nonpositive values of the vorticity component ω_z and which could of course be expected from the wind directions. It is seen from the pictures that the vorticity is highest (in absolute value) at $y = \frac{b}{2}$ and decreases with x, indicating the most spinning motion at the western boundary as well. Since the flux between any two streamlines is constant and distance between them around the western boundary decreases, the flux density must increase heavily: the flow velocity therefore also becomes a lot higher around the western boundary. This could also be observed directly from the increased density of streamlines: $v_y = -\frac{\partial \psi}{\partial x}$, which is proportional to the density of the contour lines of ψ.

We were able to solve the equations of the Stommel model analytically by the method of separation of variables since they neglect the nonlinearity in $\boldsymbol{V} \cdot \nabla \boldsymbol{V}$. When this nonlinearity is added again, we need more sophisticated methods to solve the model. Chapter 8 presents a way to do so. Another way for solving for the nonlinearity is by the numerical method of finite differences. Also, we used a rectangular domain to solve the equations on, which made it possible to give an exact solution to the boundary value problem easily. A curved boundary makes finding an exact solution a lot harder or even impossible.

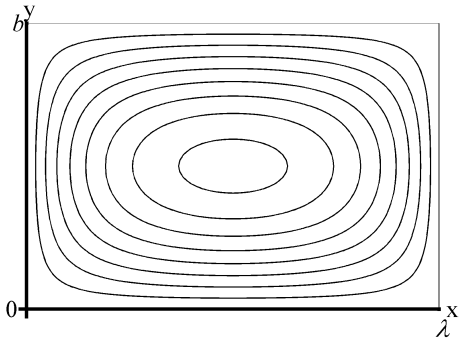

(a) *Contour plot of the stream function* ψ.

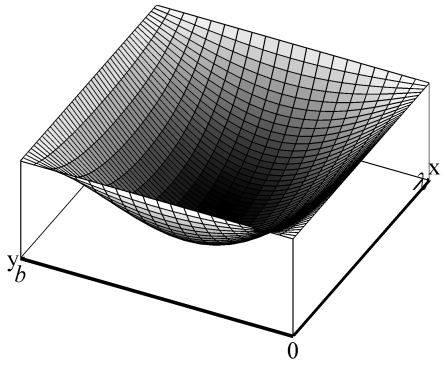

(b) *Surface plot of the stream function* ψ.

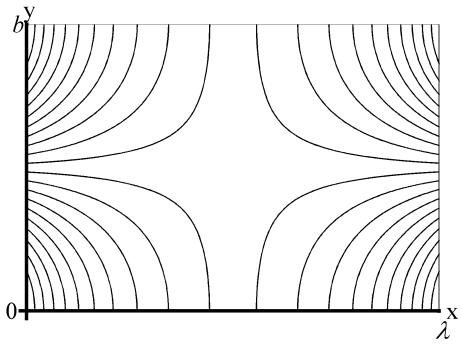

(c) *Contour plot of the height function h.*

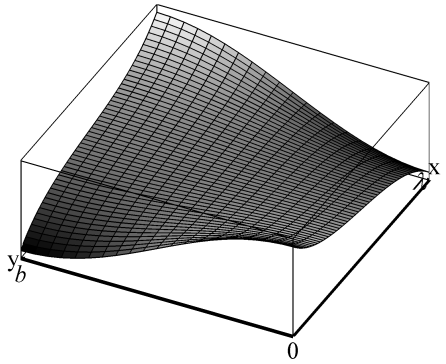

(d) *Surface plot of the height function h.*

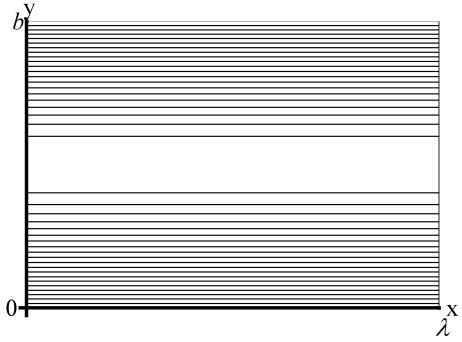

(e) *Contour plot of the vorticity component* ω_z.

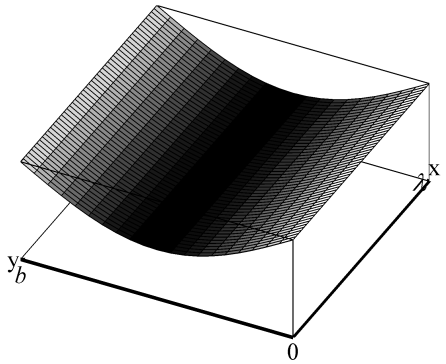

(f) *Surface plot of the vorticity component* ω_z.

Figure 5.: *Contour and surface plots of* ψ*, h and* ω_z *in a non-rotating system* ($\Omega = 0$)*. The contour plot of* ψ *gives the streamlines of the fluid flow. The density of the streamlines gives the velocity. A rotation around the center of the basin over* $180°$ *leaves the function values intact.*

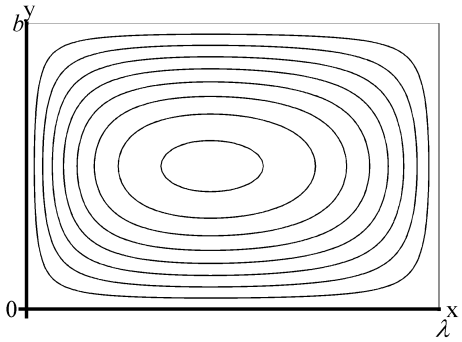

(a) *Contour plot of the stream function* ψ.

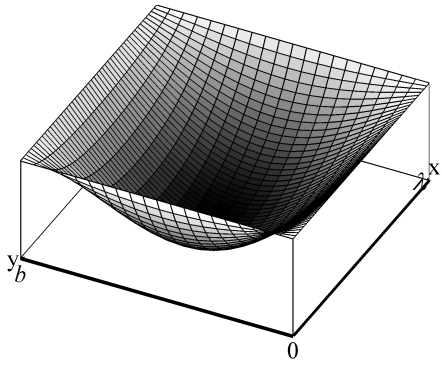

(b) *Surface plot of the stream function* ψ.

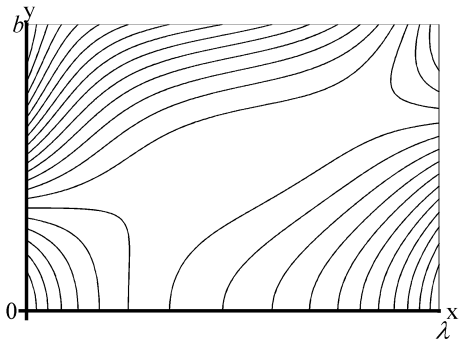

(c) *Contour plot of the height function h.*

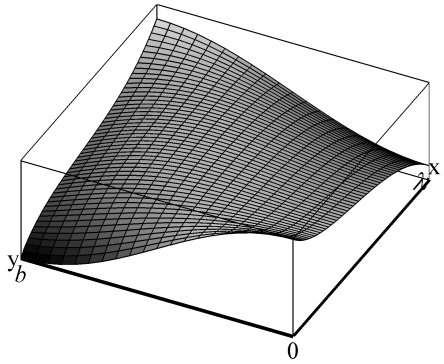

(d) *Surface plot of the height function h.*

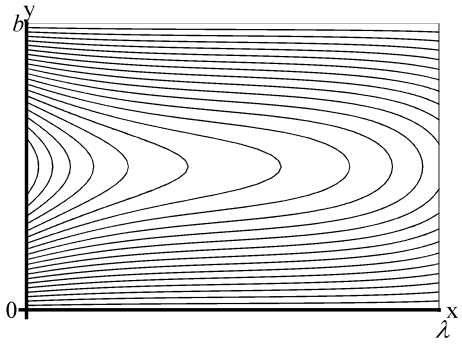

(e) *Contour plot of the vorticity component* ω_z.

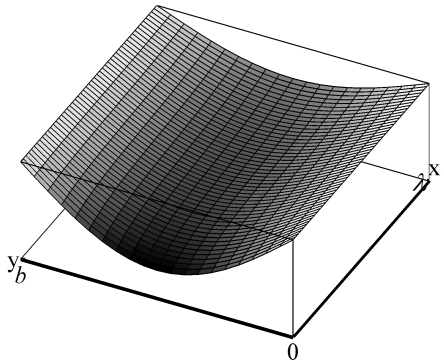

(f) *Surface plot of the vorticity component* ω_z.

Figure 6.: *Contour and surface plots of* ψ*, h and* ω_z *in a rotating system* ($\Omega = \frac{2\pi}{60 \cdot 60 \cdot 24}\ s^{-1}$*, Earth's angular velocity). The contour plot of* ψ *gives the streamlines of the fluid flow. The density of the streamlines gives the velocity.*

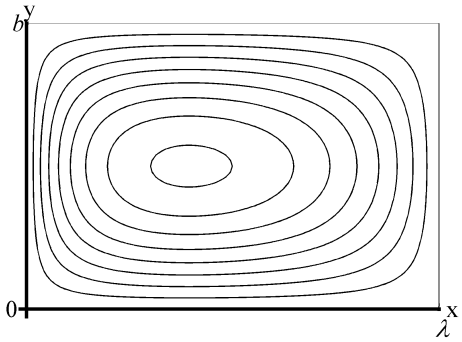

(a) *Contour plot of the stream function* ψ.

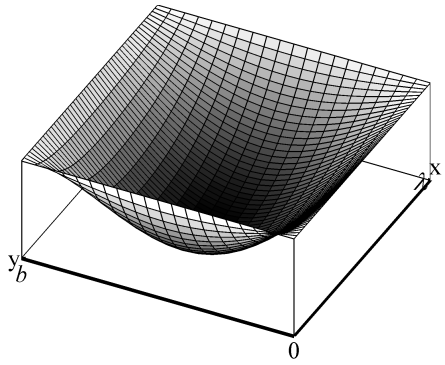

(b) *Surface plot of the stream function* ψ.

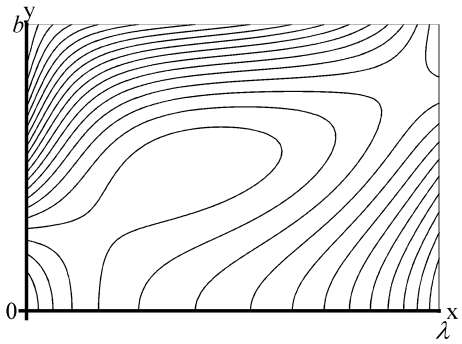

(c) *Contour plot of the height function h.*

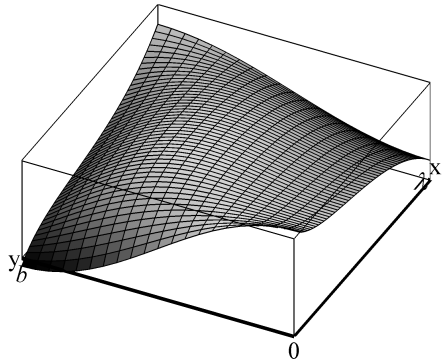

(d) *Surface plot of the height function h.*

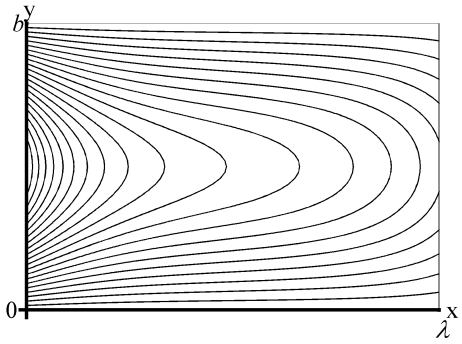

(e) *Contour plot of the vorticity component* ω_z.

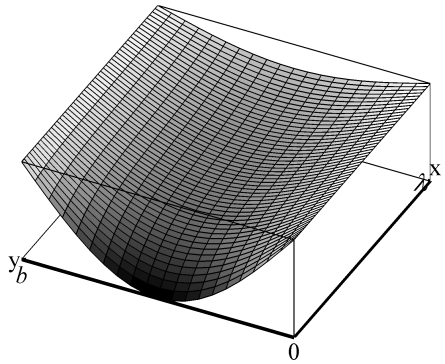

(f) *Surface plot of the vorticity component* ω_z.

Figure 7.: *Contour and surface plots of* ψ*, h and* ω_z *in a rotating system (*$\Omega = \frac{4\pi}{60 \cdot 60 \cdot 24}\ s^{-1}$*, twice Earth's angular velocity). The contour plot of* ψ *gives the streamlines of the fluid flow. The density of the streamlines gives the velocity.*

8

THE MUNK MODEL AND PEDLOSKY'S DERIVATION

The model presented by Walter Munk in [6] slightly differs from the model presented by Stommel, though their derivations can be done quite similar. In [4] and [8], this derivation is given and we will follow these publications in the derivation we present in this chapter. The procedure can easily be extended to give solutions that are more exact.

8.1 THE MUNK MODEL

The Munk model consists of a fourth order partial differential equation and a sufficient set of boundary conditions. The equation derived by Munk is

$$A\Delta(\Delta\psi) - \beta\frac{\partial\psi}{\partial x} = -(\nabla\times\boldsymbol{\tau})_3, \tag{8.1}$$

where $(\nabla\times\boldsymbol{\tau})_3$ (the z-element of the curl of $\boldsymbol{\tau} = (\tau_1,\tau_2,\tau_3)^t$, a term due to surface influence of the wind) equals $\frac{\partial\tau_2}{\partial x} - \frac{\partial\tau_1}{\partial y}$, and A represents the molecular viscosity of the flow. Note that the main difference between the Stommel and Munk models lies in the origin of the counteracting friction. The Stommel model assumes the bottom friction to be the only counteracting force, giving a term $R\Delta\psi$, while he neglects viscosity. On the other hand, Munk models the viscosity, which was neglected by Stommel, to preventing relative speeds from going to infinity, in a term $A\Delta(\Delta\psi)$, neglecting any bottom friction.

The boundary conditions that Munk imposes are the Dirichlet and Neumann conditions

$$\psi|_{\partial B} = 0, \qquad (\nabla\psi\cdot\boldsymbol{n})|_{\partial B} = 0, \tag{8.2}$$

where B is the domain, ∂B its boundary and $\boldsymbol{n}$ a unit vector normal to the boundary.

The equation that was derived by Munk is a special case of the more general equation from the derivation of Joseph Pedlosky in [8], which we tried to explain below.

For his derivation, Pedlosky uses the equations of fluid dynamics where the vertical velocity is neglected. He used a version that includes a friction term $-R\boldsymbol{V}$ just as in the Stommel model, such that the equations are

$$\frac{\partial v_x}{\partial t} + v_x\frac{\partial v_x}{\partial x} + v_y\frac{\partial v_x}{\partial y} - fv_y = -\frac{1}{\rho_0}\frac{\partial p}{\partial x} - Rv_x + A\Delta v_x + F_1, \tag{8.3a}$$

$$\frac{\partial v_y}{\partial t} + v_x\frac{\partial v_y}{\partial x} + v_y\frac{\partial v_y}{\partial y} + fv_x = -\frac{1}{\rho_0}\frac{\partial p}{\partial y} - Rv_y + A\Delta v_y + F_2, \tag{8.3b}$$

$$0 = -\frac{1}{\rho_0}\frac{\partial p}{\partial z} - g \tag{8.3c}$$

and

$$0 = \frac{\partial v_x}{\partial x} + \frac{\partial v_y}{\partial y}. \tag{8.3d}$$

We again know about the existence of a stream function $\psi(x,y,t)$ such that $v_x = \frac{\partial \psi}{\partial y}$ and $v_y = -\frac{\partial \psi}{\partial x}$. If we substitute this into the above equations, differentiate Equation 8.3a with respect to y and 8.3b with respect to x, and subtract them from each other, we find

$$\Delta\psi_t + \beta\psi_x + \psi_y\Delta\psi_x - \psi_x\Delta\psi_y = A\Delta(\Delta\psi) + (F_1)_y - (F_2)_x - R\Delta\psi. \tag{8.4}$$

The diffusion term $A\Delta(\Delta\psi)$ does not actually appear in Pedlosky's derivation in [8] but is added in [4] in order to make the derivation suit the model of Munk. The term $(F_1)_y - (F_2)_x - R\Delta\psi$ is comparable to the right-hand side of Equation 7.7 of the Stommel model, where R was considered to be part of $\boldsymbol{F}$. We let $(F_1)_y - (F_2)_x$ be equal to the surface influence of wind

$$(F_1)_y - (F_2)_x = -\frac{\tau}{\rho_0 D}, \tag{8.5}$$

with D the depth of the basin as in the Stommel model. In [4], the notation of a Jacobian matrix is used to express

$$\psi_y\Delta\psi_x - \psi_x\Delta\psi_y = -J(\psi,\Delta\psi), \tag{8.6}$$

giving

$$\Delta\psi_t + \beta\psi_x - J(\psi,\Delta\psi) = A\Delta(\Delta\psi) - \frac{\tau}{\rho_0 D} - R\Delta\psi. \tag{8.7}$$

Using the right definition of τ, setting $R = 0$, ignoring time dependence and approximating $J(\psi,\Delta\psi)$ to be zero, we find exactly Munk's model.

Similarly, defining τ right, letting $\beta = \alpha R$, $A = 0$ and ignoring both time dependence and $J(\psi,\Delta\psi)$, we find the equation of Stommel's model.

In both [4] and [8], a non-dimensionalisation method is used, from which a dimensionless differential equation is found:

$$\Delta\Psi_t + \Psi_x - Ro\cdot J(\Psi,\Delta\Psi) = A\Delta(\Delta\Psi) - T - \delta\Delta\Psi. \tag{8.8}$$

Ro in this equation is called the *Rossby number*, Ψ is the non-dimensional stream function and all derivatives are with respect to non-dimensional variables.

When $Ro = 0$, the differential equation is linear and a solution is found relatively easily. Pedlosky makes use of this fact by assuming *Ro* to be small and expressing Ψ as a series expansion around $Ro = 0$. The boundary conditions from Equation 8.2 are applied, where

$$B = \{(x,y)|0 < x < \lambda; 0 < y < b\},$$

as in the Stommel model. The Neumann condition is only required when $A \neq 0$. The solution is written as

$$\Psi(x,y,t) = \sum_{i=0}^{\infty} Ro^i \Psi_i(x,y,t). \tag{8.9}$$

As will become clear below, Ψ_n can be solved by induction from $\Psi_0, \ldots, \Psi_{n-1}$. The expansion of the derivatives of Ψ is trivial, however $J(\Psi, \Delta\Psi)$ has a more complicated series expansion:

$$\begin{aligned} J(\Psi,\Delta\Psi) &= \sum_{i=0}^{\infty} Ro^i (\Psi_i)_x \sum_{i=0}^{\infty} Ro^i (\Delta\Psi_i)_y - \sum_{i=0}^{\infty} Ro^i (\Psi_i)_y \sum_{i=0}^{\infty} Ro^i (\Delta\Psi_i)_x \\ &= J(\Psi_0,\Delta\Psi_0) + Ro[J(\Psi_1,\Delta\Psi_0) + J(\Psi_0,\Delta\Psi_1)] + \ldots \\ &= \sum_{i=0}^{\infty} \left[Ro^i \sum_{k=0}^{i} J(\Psi_k, \Delta\Psi_{i-k}) \right], \end{aligned} \tag{8.10}$$

giving as differential equation

$$\sum_{i=0}^{\infty} Ro^i \left((\Delta\Psi_i)_t + \delta\Delta\Psi_i + (\Psi_i)_x - A\Delta(\Delta\Psi_i) \right) \;=\; -T \;+\; \sum_{i=0}^{\infty} \left[Ro^{i+1} \sum_{k=0}^{i} J(\Psi_k, \Delta\Psi_{i-k}) \right]. \tag{8.11}$$

Grouping all by powers of *Ro*, we find the equations

$$(\Delta\Psi_0)_t + \delta\Delta\Psi_0 + (\Psi_0)_x - A\Delta(\Delta\Psi_0) = -T, \tag{8.12a}$$

$$(\Delta\Psi_1)_t + \delta\Delta\Psi_1 + (\Psi_1)_x - A\Delta(\Delta\Psi_1) = J(\Psi_0,\Delta\Psi_0), \tag{8.12b}$$

$$(\Delta\Psi_2)_t + \delta\Delta\Psi_2 + (\Psi_2)_x - A\Delta(\Delta\Psi_2) = \sum_{k=0}^{1} J(\Psi_k, \Delta\Psi_{1-k}), \tag{8.12c}$$

$$\vdots \qquad\qquad \vdots$$

$$(\Delta\Psi_n)_t + \delta\Delta\Psi_n + (\Psi_n)_x - A\Delta(\Delta\Psi_n) = \sum_{k=0}^{n-1} J(\Psi_k, \Delta\Psi_{n-1-k}), \tag{8.12n}$$

$$\vdots \qquad\qquad . \qquad\qquad \vdots$$

From the first of these equations, when a sufficient amount of boundary and initial value conditions is applied, Ψ_0 can be determined. After this is done, Ψ_0 can be inserted into the right-hand side of 8.12b to find Ψ_1, etc..

The *zeroth-order approximation* is $\Psi(x,y,t) = \Psi_0(x,y,t)$, of which form are both the Stommel en Munk models. A probably more accurate approximation is the *first-order approximation* $\Psi = \Psi_0 + Ro\Psi_1$, and even more details could be uncovered when considering higher orders.

In Equations 7.3 we ignored the term $\frac{DV}{Dt}$ in order to arrive at linear equations. If however we add this term, we get equations

$$v_x\frac{\partial v_x}{\partial x}+v_y\frac{\partial v_x}{\partial y}-fv_y=-\frac{1}{\rho_0}\frac{\partial p}{\partial x}+F_x, \tag{8.13a}$$

$$v_x\frac{\partial v_y}{\partial x}+v_y\frac{\partial v_y}{\partial y}+fv_x=-\frac{1}{\rho_0}\frac{\partial p}{\partial y}+F_y, \tag{8.13b}$$

$$0=-\frac{1}{\rho_0}\frac{\partial p}{\partial z}+F_z, \tag{8.13c}$$

and

$$0=\frac{\partial v_x}{\partial x}+\frac{\partial v_y}{\partial y}. \tag{8.13d}$$

This leads to the differential equation

$$\Delta\psi+\alpha\frac{\partial\psi}{\partial x}-\frac{D}{R}J(\psi,\Delta\psi)=\gamma\sin\frac{\pi y}{b}, \tag{8.14}$$

where $J(\psi,\Delta\psi)$ is the Jacobian determinant

$$J(\psi,\Delta\psi)=\begin{vmatrix}\psi_x & \Delta\psi_x\\ \psi_y & \Delta\psi_y\end{vmatrix}.$$

After non-dimensionalizing, we find the differential equation

$$\delta\Delta\Psi+\Psi_x-Ro\cdot J(\Psi,\Delta\Psi)=\sin\pi y'. \tag{8.15}$$

This differential equation leads to a system of equations such as Equations 8.12:

$$\delta\Delta\Psi_0+(\Psi_0)_x=\sin\pi y', \tag{8.16a}$$

$$\delta\Delta\Psi_1+(\Psi_1)_x=J(\Psi_0,\Delta\Psi_0), \tag{8.16b}$$

$$\delta\Delta\Psi_2+(\Psi_2)_x=\sum_{k=0}^{1}J(\Psi_k,\Delta\Psi_{1-k}), \tag{8.16c}$$

$$\vdots \qquad\qquad \vdots$$

$$\delta\Delta\Psi_n+(\Psi_n)_x=\sum_{k=0}^{n-1}J(\Psi_k,\Delta\Psi_{n-1-k}), \tag{8.16n}$$

$$\vdots \qquad . \qquad \vdots$$

The total soultion becomes $\sum_{n=0}^{\infty}Ro^n\Psi_n$. We start by solving the first equation to find Ψ_0, which has a solution

$$\Psi_0(x,y)=\frac{1}{\delta\pi^2}e^{-\frac{x}{2\delta}}\sin\pi y\left(\frac{e^{\frac{\lambda'}{2\delta}}-\cosh\kappa\lambda'}{\sinh\kappa\lambda'}\sinh\kappa x+\cosh\kappa x-e^{\frac{x}{2\delta}}\right), \tag{8.17}$$

where $\kappa = \sqrt{\frac{1}{4\delta^2} + \pi^2}$, similar to the solution in the previous chapter.

Knowing Ψ_0, we may calculate $J(\Psi_0, \Delta\Psi_0)$ and from Equation 8.16b, we will then be able to find Ψ_1, etc.. This process could best be done (numerically) by a computer, since the differential equations start to become quite long from here on.

9

AN APPLICATION: MOON'S GRAVITATIONAL PULL

Where both the Munk and Stommel models do not depend on time, we can study a *time-dependent* system by considering the effect of Moon's gravitational pull, the *tidal force*. We assume the magnitude of the lunar pull to be constant and equal to

$$g_{\text{lunar}} = \frac{2G \cdot m_{\text{moon}} r_{\text{earth}}}{R^3_{\text{earth-moon}}} \approx 1 \cdot 10^{-6} \text{ ms}^{-2}.$$

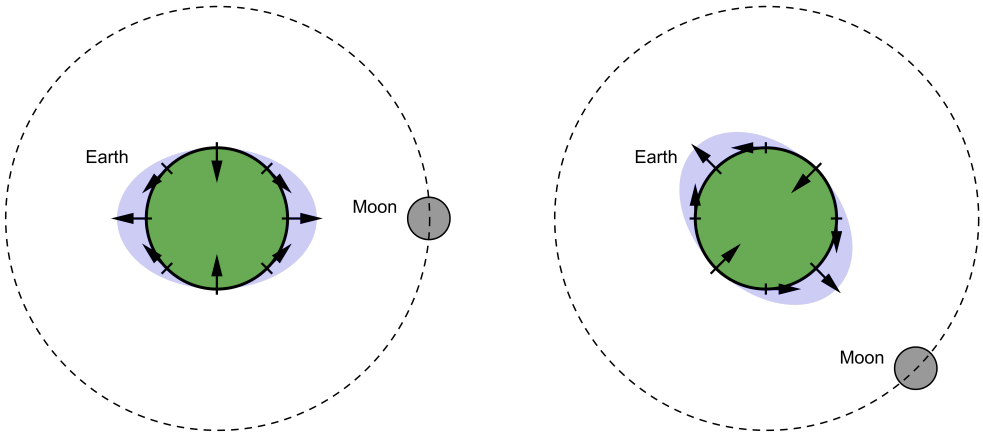

Figure 8.: *Top view of Earth (facing down on the North Pole), where direction of tidal force due to moon position is indicated at several points. The blue areas indicate the tides. Since Earth rotates in counter-clockwise direction and Moon orbits around Earth in the same direction but with a lower angular velocity, the rotation of the moon can be seen as in clockwise direction. The picture is not drawn to scale.*

We approximate the Moon to be in the same position (relative to a point on Earth) every 25 hours (so with rotational frequency $\omega = \frac{2\pi}{25 \cdot 3600}$ Hz), and consider its pull to be in the equator- or x,z-plane, such that, neglecting any initial phase, we can write for the time dependent accel-

eration, $g_{\text{lunar}}(t)$, due to lunar pull in horizontal direction[1] (see Figure 8 for an indication of the direction of the tidal force at several positions),

$$g_{\text{lunar}}(x,t) = g_{\text{lunar}} \sin(2[-\theta - \omega t])\hat{\boldsymbol{x}} \approx g_{\text{lunar}} \sin\left(-\frac{x}{\pi r_e} - 2\omega t\right)\hat{\boldsymbol{x}}, \tag{9.1}$$

where any y-dependence is neglected[2].

This gives us, besides the wind stress in the Stommel model, an additional volume force $F_{g,1} = \rho_0 \cdot g_{\text{lunar}} \sin\left(-\frac{x}{\pi r_e} - 2\omega t\right)$, while $F_{g,2} = F_{g,3} = 0$. Since $(F_{g,1})_y = (F_{g,2})_x = 0$, this additional force term does not influence the differential equation of the Stommel model. Since we are interested in time dependence here, the differential equation of the Stommel model is adapted to

$$\Delta\psi_t + R\Delta\psi + \alpha R\psi_x = AR \sin\frac{\pi y}{b}. \tag{9.2}$$

Besides the original boundary condition

$$\psi(0,y,t) = \psi(\lambda,y,t) = \psi(x,0,t) = \psi(x,b,t) = 0 \text{ for all } x,y,t, \tag{7.10}$$

another boundary condition is required now, since the differential equation has become third-order because of the term $\Delta\psi_t$. A reasonable condition is that the average net flow through the boundary is zero. Physically, this condition implies that the amount of water inside the basin is constant and thus, under the assumption of constant density, that the water height averaged over the entire basin is constant in time.

The time-independent particular solution is still a valid solution for this equation. The same holds for the time-independent homogeneous solutions, but we try to add time dependence to them, again by separation of variables: we assume $\psi_h(x,y,t) = F(x)G(y)H(t)$ to be a such a solution. Inserting it into the homogeneous differential equation

$$\Delta(\psi_h)_t + R\Delta\psi_h + \alpha R(\psi_h)_x = 0. \tag{9.3}$$

gives

$$[F''G + FG'']H' + R[F''G + FG'']H + \alpha RF'GH = 0, \tag{9.4}$$

or

$$\frac{H'}{H} = -\frac{R[F''G + FG''] + \alpha RF'G}{[F''G + FG'']} = \text{constant}. \tag{9.5}$$

From this we can solve for H, finding $H(t) = H_0 e^{Ct}$, where $C = \frac{H'}{H}$. Since terms in the differential equation are periodic, we expect our solution to be periodic as well and so we need C to be purely imaginary. Therefore, for F and G we arrive at the differential equation

$$F''(x)G(y) + F(x)G''(y) + \chi F'(x)G(y) = 0, \tag{9.6}$$

1 For some background on tidal forces, see for instance [5, p. 471-477] and Fig. 10.14 from that book. We neglect any vertical component of the tidal force since gravity is much stronger.

2 Actually, the amplitude of the tidal force is only equal to g_{lunar} when $\frac{x}{\pi r_e} - 2\omega t$, and at other places on the earth surface it is a bit smaller. However, it is of the same order of magnitude as g_{lunar} and for simplicity we stick to the round value mentioned above.

where $\chi := \alpha\frac{R}{C+R}$. This equation is similar to Equation 7.13.

We again can rewrite this to the form

$$\frac{F''(x)+\chi F'(x)}{F(x)} = -\frac{G''(y)}{G(y)} = \beta^2 > 0,$$

and we find solutions in a similar manner as before that are of the form

$$\psi_h(x,y,t) = e^{Ct-\frac{\alpha}{2}x}\left(a_1\sinh\kappa x + a_2\cosh\kappa x\right)\left[b_1\sin\beta y + b_2\cos\beta y\right], \tag{9.7}$$

where κ is now defined as $\kappa = \sqrt{\frac{\chi^2}{4}+\beta^2}$. By the boundary conditions we know that $G(0) = G(b) = 0$, such that again $b_2 = 0$ and β must have one of the values $\beta_k = \frac{k\pi}{b}$ where k is an integer that can be chosen to be positive. This can be rewritten to

$$\psi(x,y) = e^{-\frac{\alpha}{2}x}\sum_{C,k=1}^{\infty}\left[e^{Ct}\sin(\beta_k y)\left(A_{C,k}\sinh\kappa_{C,k}x + B_{C,k}\cosh\kappa_{C,k}x\right)\right] - \gamma\frac{b^2}{\pi^2}\sin\frac{\pi y}{b}. \tag{9.8}$$

If we imply the condition $\psi(0,y,t) = 0$, we find that

$$\sum_{C,k=1}^{\infty}\left[B_{C,k}e^{Ct}\sin(\beta_k y)\right] - \gamma\frac{b^2}{\pi^2}\sin\frac{\pi y}{b} = 0$$

for all y,t, such that by the time-independence of the term $-\gamma\frac{b^2}{\pi^2}\sin\frac{\pi y}{b}$, $B_{C,i} = 0$ for $C \neq 0$. We thus find $B_{C=0,k=1} = \gamma\frac{b^2}{\pi^2}$, and $B_{C,i} = 0$ for $i > 1$, as in the time-independent case.

Similarly, the coefficients $A_{C,k}$ are found to be

$$A_{C,k} = \begin{cases} \gamma\frac{b^2}{\pi^2}\frac{e^{\frac{\alpha}{2}\lambda}-\cosh\kappa_{0,1}\lambda}{\sinh\kappa_{0,1}\lambda} & C = 0, k = 1 \\ 0 & \text{else} \end{cases}.$$

The resulting *time-dependent* stream function apparently equals the *time-independent* solution we found in Chapter 7: apparently the fluid trajectories/streamlines and also the flow velocities are not influenced by the tides, which is a quite remarkable result.

The time-dependent versions of Equations 7.6 now become, when the components of $\boldsymbol{V}$ are expressed as derivatives of ψ,

$$f\psi_x = -g\frac{\partial h}{\partial x} - \frac{R}{D}\psi_y - \frac{T}{D}\cos\frac{\pi y}{b} + g_{lunar}\sin\left(-\frac{x}{\pi r_e} - 2\omega t\right), \tag{9.9a}$$

$$f\psi_y = -g\frac{\partial h}{\partial y} + \frac{R}{D}\psi_x. \tag{9.9b}$$

Equation 9.9b is the same as in the time-independent case, such that $\frac{\partial h}{\partial y}$ is independent of t and thus all time dependence is caught into the term $C(x,t)$ that appears in the time-dependent version of Equation 7.22. We find

$$\frac{\partial}{\partial x}C(x,t) = \frac{g_{\text{lunar}}}{g}\sin\left(-\frac{x}{\pi r_e} - 2\omega t\right), \tag{9.10}$$

such that

$$C(x,t) = \pi r_e \frac{g_{\text{lunar}}}{g} \cos\left(-\frac{x}{\pi r_e} - 2\omega t\right) + c(t), \tag{9.11}$$

where $c(t)$ only depends on time. Since the density, ρ_0, is assumed to be constant, we also need the volume of the sea, and thus the average of h, to be constant. Therefore, we integrate $C(x,t) - c(t)$ over the whole basin[3] and find $c(t)$ up to a constant to be

$$c(t) = -\frac{1}{\lambda b} \int_{x=0}^{x=\lambda} \int_{y=0}^{y=b} \pi r_e \frac{g_{\text{lunar}}}{g} \cos\left(-\frac{x}{\pi r_e} - 2\omega t\right) dxdy \tag{9.12}$$

$$= \frac{\pi^2 r_e^2}{\lambda} \frac{g_{\text{lunar}}}{g} \left[\sin\left(-\frac{\lambda}{\pi r_e} - 2\omega t\right) + \sin 2\omega t\right]. \tag{9.13}$$

The full height function is now found to be

$$\begin{aligned} h(x,y,t) = -\frac{b^2}{\pi^2} \frac{T\alpha}{gD} e^{-\frac{\alpha}{2}x} \Bigg[& \frac{\pi y}{b} \sin\frac{\pi y}{b} \cdot (B \sinh \kappa x + \cosh \kappa x - e^{\frac{\alpha}{2}x}) \\ & + \cos\frac{\pi y}{b} \cdot \left(\frac{1}{2}(B \sinh \kappa x + \cosh \kappa x) + \frac{\kappa}{\alpha}(B \cosh \kappa x + \sinh \kappa x) - e^{\frac{\alpha}{2}x}\right) \Bigg] \\ & + \pi r_e \frac{g_{\text{lunar}}}{g} \cos\left(-\frac{x}{\pi r_e} - 2\omega t\right) \\ & + \frac{\pi^2 r_e^2}{\lambda} \frac{g_{\text{lunar}}}{g} \left[\sin\left(-\frac{\lambda}{\pi r_e} - 2\omega t\right) + \sin 2\omega t\right]. \end{aligned} \tag{9.14}$$

For small λ, the term $\frac{x}{\pi r_e}$ is small and thus $\cos\left(-\frac{x}{\pi r_e} - 2\omega t\right) \approx \cos(-2\omega t) = \cos 2\omega t$ for $x \in [0, \lambda]$. Furthermore, by L'Hôpital's rule

$$\lim_{\lambda \to 0} \frac{\pi r_e}{\lambda} \left[\sin\left(-\frac{\lambda}{\pi r_e} - 2\omega t\right) + \sin 2\omega t\right] = \lim_{\lambda \to 0} \cos\left(-\frac{\lambda}{\pi r_e} - 2\omega t\right) = \cos(-2\omega t) = \cos 2\omega t$$

as well, such that the time-dependence is almost cancelled for low values of λ.

When λ is increased, the term we labelled $c(t)$ converges to zero and the amplitude of the tidal waves converges to $\pi r_e \frac{g_{\text{lunar}}}{g} = 3.14 \cdot 6.24 \cdot 10^6 \cdot \frac{1 \cdot 10^{-6}}{9.81} \approx 2$ m, which is of the same order of magnitude as what is measured at the Dutch coastline (see, for instance, [9] for measurements).

Using the MATLAB code in the appendices (by running the script *StommelDiagramAnimation.m* from the Appendix), an animation can be played that shows the time-dependence. During this animation, every few seconds the value of λ is increased to show the dependence of the tides on this quantity. Remark that when $\lambda \to \infty$, $B \to -1$ while at large x, $\sinh \kappa x \approx \cosh \kappa x$, such that at large values of λ the x-dependence of the time-independent part of the height function at the eastern side of the basin disappears. The most remarkable result, however, is that the stream function, and therefore the streamlines and stream velocity, do not depend on time when

3 We only need the average of $C(x,t)$ to be constant in time, since the rest of h is by time-independence automatically constant in time.

the tidal force is in $\hat{\boldsymbol{x}}$-direction and does not depend on y. Note that in reality there is a small $\hat{\boldsymbol{y}}$-component since the rotation of the moon is not exactly contained in the equator plane. Also there is some small y-dependence, such that the streamlines and flow velocities are influenced a bit.

10

SOME CONCLUDING THOUGHTS

We conclude this thesis by a short concluding chapter. Some short notes on the achievements of this work will be given. Also some current trends in physical oceanography will be discussed.

10.1 ACCOMPLISHMENTS AND ACHIEVEMENTS

According to the research proposal preceding this thesis, its goal was to study the impact of Coriolis force on the behaviour of flow particle motions. In particular, circulation problems like shallow water models of the Gulf Stream, as the Stommel model, were to be studied and solved.

In this thesis, we have read about the concepts and basic equations of fluid dynamics, the Navier-Stokes equations. We have studied the effect of Earth's rotation on large-scale systems, to find the impact of the Coriolis force on large scale fluid dynamics such as ocean flows. A simple model, the model of Henry Stommel, was used to show the effect that Coriolis force has on wind-driven ocean circulation. Using some simplifications and approximations, we were able to solve this model analytically and we found an explanation on the accumulation of stream-lines near the western boundary of wind-driven circulating ocean streams such as the Gulf Stream. The method of Joseph Pedlosky to solve more sophisticated non-linear models was explored.

Finally, in addition to the research proposal, a time-dependent adaption was made to the Stommel model, adding tidal waves to it. It appeared that the tidal movement has no effect on the streamlines and flow velocities of the ocean.

10.2 FURTHER INVESTIGATION

The models and techniques described in this thesis originate from mid-twentieth century papers and are extremely simplified approximations of reality. Nowadays computational methods and hardware have been improved a lot and more complex models can be solved easily using numerical methods. Solving the non-linear version of the Stommel model, presented in Chapter 8, numerically would be a lot easier now than it was fifty years ago and it would be good to have a look at this in future investigations. Also more realistic domains and bathymetries could be used in models, to give more accurate results.

One of the techniques used in physical oceanography over the past 50 years is including measurement data in flow models to make predictions more accurate, as is described in [4]. The other way around, these models may be used to improve measurement techniques.

More advanced ocean models also play an important role in the hot discussions about climate change, for instance in predicting the release and capture of carbon dioxide in the deep oceans or the effect of polar cap melting on the ocean streams and ocean height.

BIBLIOGRAPHY

[1] J. D. Anderson Jr. *Computational Fluid Dynamics, The Basics with Applications*. McGraw-Hill, 1995.

[2] J. D. Anderson Jr. *Fundamentals of Aerodynamics*. McGraw-Hill, 3rd edition, 2001.

[3] S. J. Colley. *Vector Calculus*. Pearson Prentice Hall, 2006.

[4] R. Malek-Madani. *Physical Oceanography: A Mathematical Introduction with MATLAB*. Taylor & Francis Group, LLC, 2012.

[5] D. Morin. *Introduction to Classical Mechanics With Problems and Solutions*. Cambridge University Press, 2009.

[6] W. H. Munk. On the wind-driven ocean circulation. *Journal of Meteorology*, 7(2):79–93, April 1950.

[7] J. Otto, editor. *Ottův slovník naučný*, volume 17. J. Otto, 1901.

[8] J. Pedlosky. A study of the time dependent ocean circulation. *Journal of Atmospheric Sciences*, 22:267–272, May 1965.

[9] Rijkswaterstaat. Waterstanden. *http://www.rijkswaterstaat.nl/images/Referentiewaarden%20waterstanden_tcm174-326696.pdf*, s.d. [Accessed: 2015-02-06].

[10] H. Stommel. The westward intensification of wind-driven ocean currents. *Transactions, American Geophysical Union*, 29(2):202–206, April 1948.

[11] G. Veronis. Dynamics of large-scale ocean circulation. In B.Warren and C.Wunsch, editors, *Evolution of Physical Oceanography*, chapter 5, pages 140–183. Massachusetts Institute of Technology, 1981.

A

MATLAB CODES

In this appendix, several MATLAB codes are included that were used for ocean simulations.

The script *StommelDiagram.m* can be used to graph the stream functions and height functions of the Stommel model in Chapter 7. The MATLAB functions StommelStream, StommelHeight and StommelVorticity from the scripts *StommelStream.m*, *StommelHeight.m* and *StommelVorticity.m* are called in this script and calculate the values of the height and stream function.

The script *StommelDiagramAnimation.m* produces an animation of the time-dependent extended Stommel model from Chapter 9 and calls *StommelHeightT.m* to calculate the time-dependent height.

Some of the scripts make use of the plugin *oaxes* which can be found on the internet. Also a picture of a compass rose, called *wind.jpg* is used.

StommelDiagram.m

```
% StommelDiagram.m
% Rik Ledoux, 2015
% This script creates diagrams showing contour and surface
   plots of the
% streamfunction and heightfunction from the Stommel model.

%% definition of relevant constants
lambda=10^7; % x-dimension
b=2*pi*10^6; % y-dimension
dx1=1000000/5; % x-step for the surface plots
dy1=2*pi*1000000/20; % y-step for the surface plots
dx2=1000000/50; % x-step for the contour plots
dy2=2*pi*1000000/50; % y-steps for the contour plots
T=0.1; % wind stress factor
Omega=2*pi/(60*60*24); % rotational frequency
[X,Y]=meshgrid(0:dx1:lambda,0:dy1:b);
[X2,Y2]=meshgrid(0:dx2:lambda,0:dy2:b);
clf
%% calculation of streamfunction values
```

```
 Z=StommelStream(X,Y,lambda,b,T,Omega);
 Z2=StommelStream(X2,Y2,lambda,b,T,Omega);
%% surface plot of the streamfunction
subplot(3,2,1)
surf(X,Y,Z)
% the code below is to make-up the plot
view([-2,-1,4])
hold on
oaxes([0 0 -10^7],'ZAxisLine','off','XTickMode','manual','
   YTickMode','off','ZTickMode','off','XLabel',{'0', '\fontname
   {Times} x'},'YLabel',{'', '\fontname{Times} y'},'Zlabel',{''
   ,''},'XTick',[0 lambda],'XTickLabel',{'\fontname{Times} 0',
   '\fontname{Times} \it{\lambda}'},'YTick',[0 b],'YTickLabel'
   ,{'\fontname{Times} 0', '\fontname{Times} \it{b}'},'Arrow','
   off')
axis off
grid off
axis([0 lambda 0 b -0.84*10^7 0])
plot3([0 lambda lambda 0 0],[0 0 b b 0],[0,0,0,0,0]-0.84*10^7,
   'k')
plot3([0 lambda lambda 0 0],[0 0 b b 0],[0,0,0,0,0]+0,'k')
plot3([ 0 0],[b b],[-0.84*10^7 0],'k')
plot3([ lambda lambda],[b b],[-0.84*10^7 0],'k')
plot3([ 0 0],[0 0],[-0.84*10^7 0],'k')
plot3([ 0 0]+lambda,[0 0],[-0.84*10^7 0],'k')
colormap gray
hold off
%% contour plot of the streamfunction
subplot(3,2,2)
[C,h]=contour(X2,Y2,Z2,'k');
% the code below is to make-up the plot
axis([0-200000 lambda+1 -200000 +b+10])
oaxes([0 0 -10^7],'ZAxisLine','off','XTickMode','manual','
   YTickMode','off','ZTickMode','off','XLabel',{'0', '\fontname
   {Times} x'},'YLabel',{'', '\fontname{Times} y'},'Zlabel',{''
   ,''},'XTick',[0 lambda],'XTickLabel',{'\fontname{Times} 0',
   '\fontname{Times} \it{\lambda}'},'YTick',[0 b],'YTickLabel'
   ,{'\fontname{Times} 0', '\fontname{Times} \it{b}'},'Arrow','
   off')
hold on
axis off
grid off
```

```
plot([0 0 lambda lambda 0],[0 b b 0 0],'k')
hold off
%% calculation of the height function values
Z=StommelHeight(X,Y,lambda,b,T,Omega);
Z2=StommelHeight(X2,Y2,lambda,b,T,Omega);
%% surface plot of the height function
subplot(3,2,3)
surf(X,Y,Z)
% the code below is to make-up the plot
view([-2,-1,4])
hold on
oaxes([0 0 -10^7],'ZAxisLine','off','XTickMode','manual','
   YTickMode','off','ZTickMode','off','XLabel',{'0', '\fontname
   {Times} x'},'YLabel',{'', '\fontname{Times} y'},'Zlabel',{''
   ,''},'XTick',[0 lambda],'XTickLabel',{'\fontname{Times} 0',
   '\fontname{Times} \it{\lambda}'},'YTick',[0 b],'YTickLabel'
   ,{'\fontname{Times} 0', '\fontname{Times} \it{b}'},'Arrow','
   off')
axis off
grid off
axis([0 lambda 0 b -120. 120.])
plot3([0 lambda lambda 0 0],[0 0 b b 0],[0,0,0,0,0]-120.0,'k')
plot3([0 lambda lambda 0 0],[0 0 b b 0],[0,0,0,0,0]+120.0,'k')
plot3([ 0 0],[b b],[-120.0 120.0],'k')
plot3([ lambda lambda],[b b],[-120.0 120.0],'k')
plot3([ 0 0],[0 0],[-120.0 120.0],'k')
plot3([ 0 0]+lambda,[0 0],[-120.0 120.0],'k')
hold off
colormap gray
%% contour plot of height function
subplot(3,2,4)
[C,h]=contour(X2,Y2,Z2,20,'k');
% the code below is to make-up the plot
axis([0-200000 lambda+1 0-200000 b+10])
oaxes([0 0 -10^7],'ZAxisLine','off','XTickMode','manual','
   YTickMode','off','ZTickMode','off','XLabel',{'0', '\fontname
   {Times} x'},'YLabel',{'', '\fontname{Times} y'},'Zlabel',{''
   ,''},'XTick',[0 lambda],'XTickLabel',{'\fontname{Times} 0',
   '\fontname{Times} \it{\lambda}'},'YTick',[0 b],'YTickLabel'
   ,{'\fontname{Times} 0', '\fontname{Times} \it{b}'},'Arrow','
   off')
hold on
```

```
axis off
grid off
plot([0 0 lambda lambda 0],[0 b b 0 0],'k')
hold off
%% calculation of the vorticity function values
Z=StommelVorticity(X,Y,lambda,b,T,Omega);
Z2=StommelVorticity(X2,Y2,lambda,b,T,Omega);
%% surface plot of the vorticity function
subplot(3,2,5)
surf(X,Y,Z)
% the code below is to make-up the plot
view([-2,-1,4])
hold on
oaxes([0 0 -10^7],'ZAxisLine','off','XTickMode','manual','
   YTickMode','off','ZTickMode','off','XLabel',{'0', '\fontname
   {Times} x'},'YLabel',{'', '\fontname{Times} y'},'Zlabel',{''
   ,''},'XTick',[0 lambda],'XTickLabel',{'\fontname{Times} 0',
   '\fontname{Times} \it{\lambda}'},'YTick',[0 b],'YTickLabel'
   ,{'\fontname{Times} 0', '\fontname{Times} \it{b}'},'Arrow','
   off')
axis off
grid off
axis([0 lambda 0 b -5*10^-6 0])
plot3([0 lambda lambda 0 0],[0 0 b b 0],[0,0,0,0,0]-5*10^-6,'k
   ')
plot3([0 lambda lambda 0 0],[0 0 b b 0],[0,0,0,0,0]+0,'k')
plot3([ 0 0],[b b],[-5*10^-6 0],'k')
plot3([ lambda lambda],[b b],[-5*10^-6 0],'k')
plot3([ 0 0],[0 0],[-5*10^-6 0],'k')
plot3([ 0 0]+lambda,[0 0],[-5*10^-6 0],'k')
hold off
colormap gray
%% contour plot of vorticity function
subplot(3,2,6)
[C,h]=contour(X2,Y2,Z2,20,'k');
% the code below is to make-up the plot
axis([0-200000 lambda+1 0-200000 b+10])
oaxes([0 0 -10^7],'ZAxisLine','off','XTickMode','manual','
   YTickMode','off','ZTickMode','off','XLabel',{'0', '\fontname
   {Times} x'},'YLabel',{'', '\fontname{Times} y'},'Zlabel',{''
   ,''},'XTick',[0 lambda],'XTickLabel',{'\fontname{Times} 0',
   '\fontname{Times} \it{\lambda}'},'YTick',[0 b],'YTickLabel'
```

```
   ,{'\fontname{Times} 0', '\fontname{Times} \it{b}'},'Arrow','
   off')
hold on
axis off
grid off
plot([0 0 lambda lambda 0],[0 b b 0 0],'k')
hold off
```

StommelStream.m

```
% StommelStream.m
% Rik Ledoux, 2015
% A function that calculates the values of the streamfunction
   from the
% Stommel model.

function z=StommelStream(x,y,lambda,b,T,Omega)
    z=0;
    D=200;
    R=0.02;
    gamma=T*pi/(R*b);
    alpha=D/R*Omega*2.5*10^-7;
    kappa=sqrt(alpha^2/4+pi^2/(b^2));

    z=gamma*b^2/(pi^2)*exp(-alpha*x/2).*sin(pi*y/b).*((exp(
       alpha*lambda/2)-cosh(kappa*lambda))/sinh(kappa*lambda)*
       sinh(kappa*x)+cosh(kappa*x)-exp(alpha*x/2));
end
```

StommelHeight.m

```
% StommelStream.m
% Rik Ledoux, 2015
% A function that calculates the values of the height function
    from the
% Stommel model.

function z=StommelHeight(x,y,lambda,b,T,Omega)
    z=0;
    D=200;
    R=0.02;
    gamma=T*pi/(R*b);
    alpha=D/R*Omega*2.5*10^-7;
```

```
    kappa=sqrt(alpha^2/4+pi^2/(b^2));
    r=6240*1000;
    g=9.81;

    B=(exp(alpha*lambda/2)-cosh(kappa*lambda))/sinh(kappa*
       lambda);

    z=-b^2/pi^2*T*alpha/(g*D)*exp(-alpha*x/2).*(sin(pi*y/b)*pi
       .*y/b.*(B*sinh(kappa*x)+cosh(kappa*x)-exp(alpha*x/2))+
       cos(pi*y/b).*(1/2*(B*sinh(kappa*x)+cosh(kappa*x))-exp(
       alpha*x/2)+kappa/alpha*(B*cosh(kappa*x)+sinh(kappa*x))))
       ;
end
```

StommelVorticity.m

```
% StommelStream.m
% Rik Ledoux, 2015
% A function that calculates the values of the z-vorticity
   from the
% Stommel model.

function z=StommelVorticity(x,y,lambda,b,T,Omega)
    z=0;
    D=200;
    R=0.02;
    gamma=T*pi/(R*b);
    alpha=D/R*Omega*2.5*10^-7;
    kappa=sqrt(alpha^2/4+pi^2/(b^2));
    B=(exp(alpha*lambda/2)-cosh(kappa*lambda))/sinh(kappa*
       lambda);
    z=-gamma.*sin(pi*y/b).*(1+b^2/(pi^2)*exp(-alpha*x/2).*(
       alpha^2/2*(B*sinh(kappa*x)+cosh(kappa*x))-alpha*kappa*(B
       *cosh(kappa*x)+sinh(kappa*x))));
end
```

StommelDiagramAnimation.m

```
% StommelDiagram.m
% Rik Ledoux, 2015
% This script creates diagrams showing contour and surface
   plots of the
% streamfunction and heightfunction from the Stommel model.
```

```
%% definition of relevant constants
lambda0=10^7; % x-dimension
b=2*pi*10^6; % y-dimension
glunar=1*10^-6; %amplitude of the tidal force
%glunar is set to 10 times its actual value, to make
   differences visible
T=0.1; % wind stress factor
Omega=2*pi/(60*60*24); % rotational frequency
Tstep=5; % time step in hours/second
Tmax=500*3600; % maximum number of hours.
%%
clf
ii=0;

t=0;
%% loading image for bottom surface wind directions
img = 256*round(imread('wind.jpg')/256); % load the image in
   black/white
imgtra = (img==0);
zImage = [0 0; 0 0]-120;    % the z-data for the image corners
h=figure(1);
while t<Tmax
    tic
    lambda=floor(t/(3600*50)+1)*lambda0;
    dx1=lambda/80;
    dy1=b/20;
    [X,Y]=meshgrid(0:dx1:lambda,0:dy1:b);
    xImage = [0 lambda; 0 lambda]/2;    % the x-data for the
       image corners
    yImage = [b b; 0 0]/2;              % the y-data for the
       image corners
    Z=StommelHeightT(X,Y,t,lambda,b,T,Omega,glunar);
    ii=ii+1;

    surf(X,Y,Z)

    % the lines below are to markup the plot
    view([-1.2,-4.5,6])
    hold on
    set(h,'Color',[1 1 1])
    axis off
```

```
    grid off
    axis([0 lambda 0 b -120. 120.])
    plot3([0 lambda lambda 0 0],[0 0 b b 0],[0,0,0,0,0]-120.0,
       'k')
    plot3([0 lambda lambda 0 0],[0 0 b b 0],[0,0,0,0,0]+120.0,
       'k')

    plot3([ 0 0],[b b],[-120.0 120.0],'k')
    plot3([ lambda lambda],[b b],[-120.0 120.0],'k')
    plot3([ 0 0],[0 0],[-120.0 120.0],'k')
    plot3([ 0 0]+lambda,[0 0],[-120.0 120.0],'k')
    colormap(1/1.2*(1.2-gray))
    text(lambda/20,b,150,strcat('Time: ',num2str(mod(t
       /3600,50),'%10.1f'),' hours'),'FontSize',16)
    text(lambda/8,b,90,strcat('Every 50 hours, \lambda is
       increased:'),'FontSize',16)
    text(lambda/8,b,60,(strcat('\lambda =',num2str(lambda,'
       %10.0e'),' m')),'Color',[.7 0 0],'FontSize',16)
    text(lambda/8,b,30,(strcat('b =',num2str(b,' %10.0e'),' m'
       )),'FontSize',16)
    text(lambda/8,b,0,(strcat('g_{lunar} =',num2str(glunar,'
       %10.0e'),' ms^{-2}')),'FontSize',16)
    surf(xImage,yImage,zImage,'CData',img,'FaceColor','
       texturemap','EdgeColor','none');

    hold off

    pause(0.001)
    t=t+toc*3600*Tstep;
end
```

StommelHeightT.m

```
% StommelStream.m
% Rik Ledoux, 2015
% A function that calculated the values of the height function
    from the
% Stommel model.

function z=StommelHeightT(x,y,t,lambda,b,T,Omega,glunar)
    z=0;
    D=200;
    R=0.02;
```

```
    gamma=T*pi/(R*b);
    alpha=D/R*Omega*2.5*10^-7;
    kappa=sqrt(alpha^2/4+pi^2/(b^2));
    r=6240*1000;
    g=9.81;
    omega=2*pi/(25*3600);

    B=(exp(alpha*lambda/2)-cosh(kappa*lambda))/sinh(kappa*
       lambda);
    z=-b^2/pi^2*T*alpha/(g*D)*exp(-alpha*x/2).*(sin(pi*y/b)*pi
       .*y/b.*(B*sinh(kappa*x)+cosh(kappa*x)-exp(alpha*x/2))+
       cos(pi*y/b).*(1/2*(B*sinh(kappa*x)+cosh(kappa*x))-exp(
       alpha*x/2)+kappa/alpha*(B*cosh(kappa*x)+sinh(kappa*x))))
       +pi*r*glunar/g*cos(-x/(pi*r)-2*omega*t) +pi^2*r^2/lambda
       *glunar/g*(sin(-lambda/(pi*r)-2*omega*t)+sin(2*omega*t))
       ;
end
```